Hydraulic response of a tropical urban estuary to a typhoon event: case study of Ho Chi Minh City and typhoon Usagi

Francisco Rodrigues do Amaral[1], Nicolas Gratiot[1,2], and Thierry Pellarin[1]

[1]IGE, Univ. Grenoble Alpes, CNRS, IRD, 38000, Grenoble, France
[2]CARE, Ho Chi Minh City University of Technology (HCMUT), VNU-HCM, 268 Ly Thuong Kiet Street, District 10, Ho Chi Minh City, Viet Nam

Correspondence: Francisco Rodrigues do Amaral (francisco.amaral@univ-grenoble-alpes.fr)

Abstract. We investigate the most severe rainfall event ever experienced in Ho Chi Minh City (HCMC), Vietnam. It occurred on November 25th, 2018 when typhoon (TY) Usagi directly hit HCMC. During this event, there was more than 300 mm in rainfall over 24h which led to flooding and considerable material damages. We propose an in-depth study of the hydrological response of this urban estuary region at a short time scale by focusing on the days before and after typhoon Usagi. For the first
5 time in a data scarce region, satellite and in-situ measurements were gathered and jointly analyzed during an unprecedented extreme event that affected millions of people in the HCMC megalopolis. We use a set of data analysis and signal processing tools to characterize and quantify both coastal and continental effects on the hydrosystem. This approach not only allowed a thorough investigation of the typhoon's impacts but also allowed new insights on the hydrological behaviour of this region. We found that TY Usagi made landfall just south of HCMC without forming a significant storm surge. The extreme rainfall
10 brought by Usagi does not translate in immediate river discharge but presents a 10 hour time lag between peak precipitation and peak residual discharge. Nevertheless, increased water levels can be seen at both urban and upstream river stations with a similar time lag. At the upstream station, residual discharge represents 1.5 % of available rain water and evidence of upstream wide spread flooding was found. Additionally, groundwater recharging processes might have played a significant role. At the urban station, residual discharge cannot be estimated from observed water level. However, we assess the potential surface run-
15 off during the event to be 8.9 % of the upstream residual discharge. Hence, the Saigon river would be capable of evacuating the urban flood water after the event. However, a time lag in peak water level and peak rainfall was found and attributed to the combination of high tide and impervious streets which prevented the evacuation of rain water and resulted in the worst flooding happening around the urban location. Overall, it was found that despite not having a significant storm surge, the coastal tidal forcing is predominant in the hydrodynamics of the river even during severe heavy rainfall with tidal fluctuations of water level
20 and respective discharge much larger than the residuals.

1 Introduction

Potential impacts of extreme water level events on low elevation coastal zones (LECZ) are increasing as populations grow and mean sea levels rise. To better prepare for the future, a good understanding of the hydrological dynamics in tidal rivers during extreme rainfall events enables coastal engineers and managers a more reliable forecasting of extreme water levels and better

25 decision making by researchers and policy makers. Along tropical and sub-tropical regions, the most energetic forcing agents for the coast are storm systems that associate extreme winds with extreme rainfall and that result in severe physical and human damages (Haigh et al., 2014). Under the impact of global warming and climate change, concerns about such extreme weather events and their local impacts have been under the scope of scientists and governments (Haigh et al., 2014; Heidarzadeh et al., 2018; Le et al., 2019).

30 Vietnam lies within the most active cyclogenesis region in the world and 4 to 6 typhoons hit the coast every year from October to December (Thuan et al., 2016). The southern part of Vietnam has generally been perceived to be less vulnerable to typhoons compared to other parts of the country. However, a substantial amount of typhoons has approached southern Vietnam in the past even though the probability of occurrence is smaller than in the northern regions of the country (Takagi et al., 2014). The south of Vietnam consists of a LECZ associated with Ho Chi Minh City (HCMC): a mega city with a population density

35 that can reach up to 30,000 inhabitants/km^2 (Nguyen et al., 2019b). Water is ubiquitous in HCMC which is traversed by the complex Saigon river system with a network of about 800 km of watercourses and canals (Ngoc et al., 2016). Additionally, 90 % of the urban area of HCMC is impermeable and leads to strong effects on hydrological cycle (Vachaud et al., 2020). Furthermore, this leads to recurrent widespread flooding either of riverine origin or by rainfall runoff which coupled with an increase in occurrence of extreme rainfall events over HCMC (Ho et al., 2014) makes it one of the most vulnerable coastal

40 regions in the world.

On November 25th 2018, HCMC was hit by the Usagi typhoon. According to the forecast department of the Southern Centre for Hydro-Meteorological Forecasting (SCHMF), this was the highest ever recorded rainfall in a 24-hour period in the megalopolis. In Camenen et al. (2021) a monthly evaluation of the Saigon River's response to this extreme rainfall yielded a paradoxical result: a lack of direct response in both water level and discharge. However, there is a clear interest in better

45 understanding how the hydrosystem physically behaved during and just after this event at finer scales than the monthly average.

In this paper, we propose an in-depth study of the hydrological response of this urban estuary region at a short time scale by focusing on the period around typhoon Usagi. We use a set of tools to characterize and quantify both coastal and continental effects on the hydrosystem. For the first time in a data scarce region (Hoballah Jalloul et al., 2022), satellite and in-situ measurements were gathered and jointly analyzed during an unprecedented extreme event that affected millions of people in

50 the HCMC megalopolis. We go from an hydrological approach to a data analysis and signal processing approach in order to analyze coastal and river water levels, rainfall and flood. In Sect. 2, we introduce the case study by describing and characterizing the study region, Ho Chi Minh City and the Typhon Usagi. Then, Sect. 3 presents the methodologies and data that were used to characterize and quantify the impacts. Results are presented and discussed in Sect. 4 followed by a conclusion in Sect. 5.

2 Case Study: Ho Chi Minh City and Typhoon Usagi

55 Ho Chi Minh City (HCMC) is located in southern Vietnam (Fig. 1), in a low elevation coastal zone, where 65 % of its territory is at an altitude below 1.5 m above mean sea level (amsl) (Vachaud et al., 2019). It is characterized by a subtropical monsoon climate with two seasons. The rainy season extends from May to October with a heavy rain period from September to October.

The average yearly rainfall over HCMC is 2000 mm of which about 90 % is received during the wet season (Couasnon et al., 2022; Binh et al., 2019; Nguyen et al., 2019a). For a given heavy rain event, the precipitation shows a high variability at

60   short spatial scales with considerable differences from one district to another (Vachaud et al., 2019). Urban flooding due to downpours has a high impact on this megalopolis paralyzing it for several hours (Duy et al., 2017) and can already occur for events starting at 50 mm of accumulated rainfall (Vachaud et al., 2019). Together with heavy precipitation, HCMC is also affected by the combined effects of semi-diurnal tidal waves, with amplitude reaching a maximum of 4 m (Schwarzer et al., 2016), and high water discharge from the Saigon river (between -1500 m^3s^{-1} and 2000 m^3s^{-1}, Camenen et al. (2021)). The

65   Saigon river is a complex river system, subject to several human and environmental interactions before flowing into the Dong Nai River and finally, into coastal waters. The Saigon river flows from its source in Cambodia to the Dau Tieng Reservoir (270 km^2 and 1580·10^6 m^3) before passing through the HCMC megalopolis. In total, it is 225 km long and its catchment area has a surface of about 4800 km^2 (Nguyen et al., 2019b). The flow of the Saigon river is predominantly driven by tidal currents, which affect both its water level and water discharge, with regular flooding in low-lying urban districts during high spring tides. This

70   flood risk is further exacerbated due to ground subsidence and the possible impacts of upstream dams on sediment trapping (Marchesiello et al., 2019).
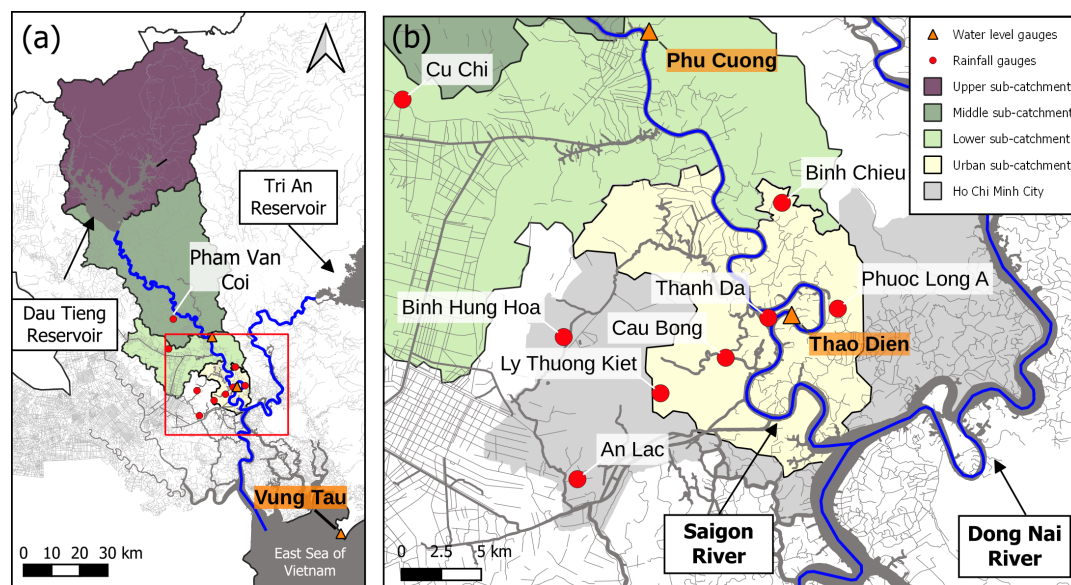
Figure 1. (a) The estuary of the Saigon-Dong Nai river system (blue). The Saigon river watershed is divided into four sub-catchments: upper, middle, lower and urban. (b) The Ho Chi Minh City center (grey) and the location of surrounding gauges. The water level gauges (orange triangles) were used for the harmonic tidal analysis and the rainfall gauges (red circles) were used for validation of gridded precipitation datasets.The Pham Van Coi rainfall gauge and the Vung Tau gauge are located outside the spatial extent of (b). The area shown in (b) is represented by the red box in (a).

The Saigon River estuary where HCMC is situated borders the East Sea of Vietnam (also known as South China Sea) one of the most active Typhoon basins in the world with about 30 % of the world's annual tropical storms occurring in this region (Trinh et al., 2020). On average, about 4-6 typhoons affect the Vietnam coast (Thuy, 2003; Thuy et al., 2016) annually. The

75 expected increase of the number and intensity of typhoons due to climate change (Lin et al., 2012) combined with the low elevation and high population density of HCMC, makes it one of the most vulnerable cities to be impacted by typhoons. In addition, the heavy rains and extreme high-water levels associated with typhoons aggravate the already high flood risk in the city. In this paper, we focus on one of the most severe rainfall events that this city has ever experienced. It occurred in November 2018, when typhoon Usagi hit HCMC. During this event, there was more than 300 mm in rainfall over 24 h which

80 led to flooding and considerable material damages.
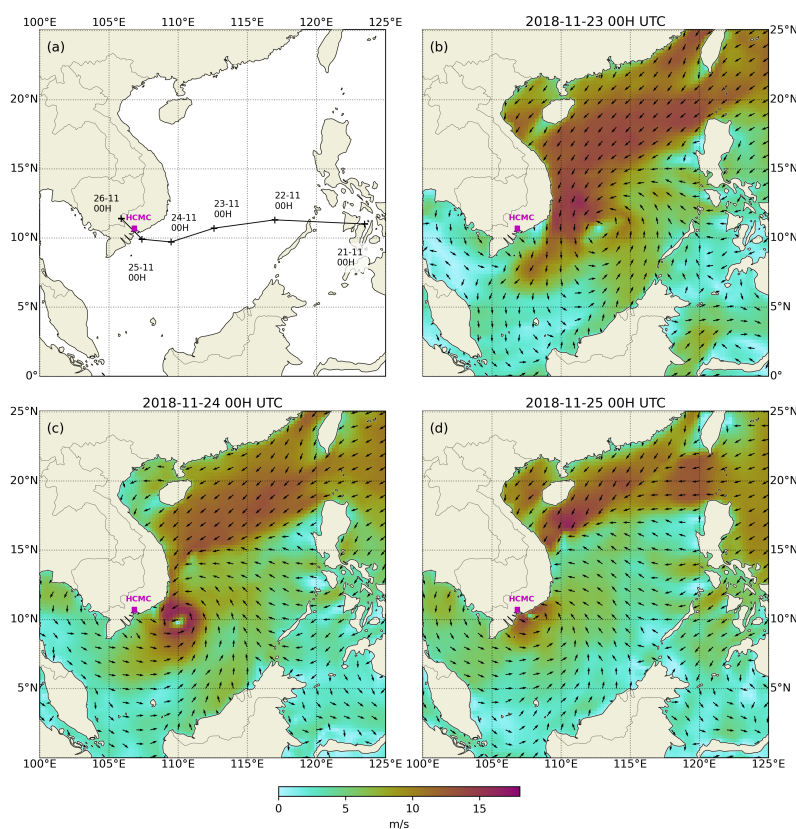
Figure 2. (a) The track of Typhoon Usagi and Ho Chi Minh City (pink); (b–d) ERA5 10-m wind fields from November 23rd, 2018 00H UTC to November 25th, 2018 00H UTC.

Typhoon Usagi was a tropical cyclone that affected the Philippines and southern Vietnam in late November 2018, causing severe damage around the Visayas region (Philippines) and Ho Chi Minh City. The storm formed from a disturbance in the Central Pacific basin on November 3rd and developed into a tropical storm (TS) three weeks later, on November 13th. Usagi underwent rapid intensification and peaked in intensity before making its final landfall on the coastal city of Vung Tau just

 south of HCMC as a weakening tropical storm on November 25th. In Fig. 2 the track of Typhoon Usagi near HCMC is shown using the lowest pressure as indicator. While never considered as a typhoon by the Japan Meteorological Agency (JMA), the Joint Typhoon Warning Center (JTWC) assessed its intensity to be equivalent to Category 2 status on the Saffir–Simpson scale. On November 25th, both the JMA and the JTWC downgraded Usagi from typhoon to a tropical storm as central convection weakened. Usagi made landfall on Vung Tau, Vietnam at 07:00 UTC as a tropical storm, with the JTWC downgrading Usagi

90 to a tropical depression later that day. During November 26th, the JMA also downgraded Usagi to a tropical depression. Usagi dissipated over Cambodia at 00:00 UTC on November 27th.

3 Methods and Data

The impact of a typhoon (TY) on an hydrological system can be separated into two main drivers: continental and coastal (Fig. 3). The first in the form of rainfall-runoff, infiltration and exfiltration influenced by topography and land use. The second in the

95 form of astronomical tide and storm surge.
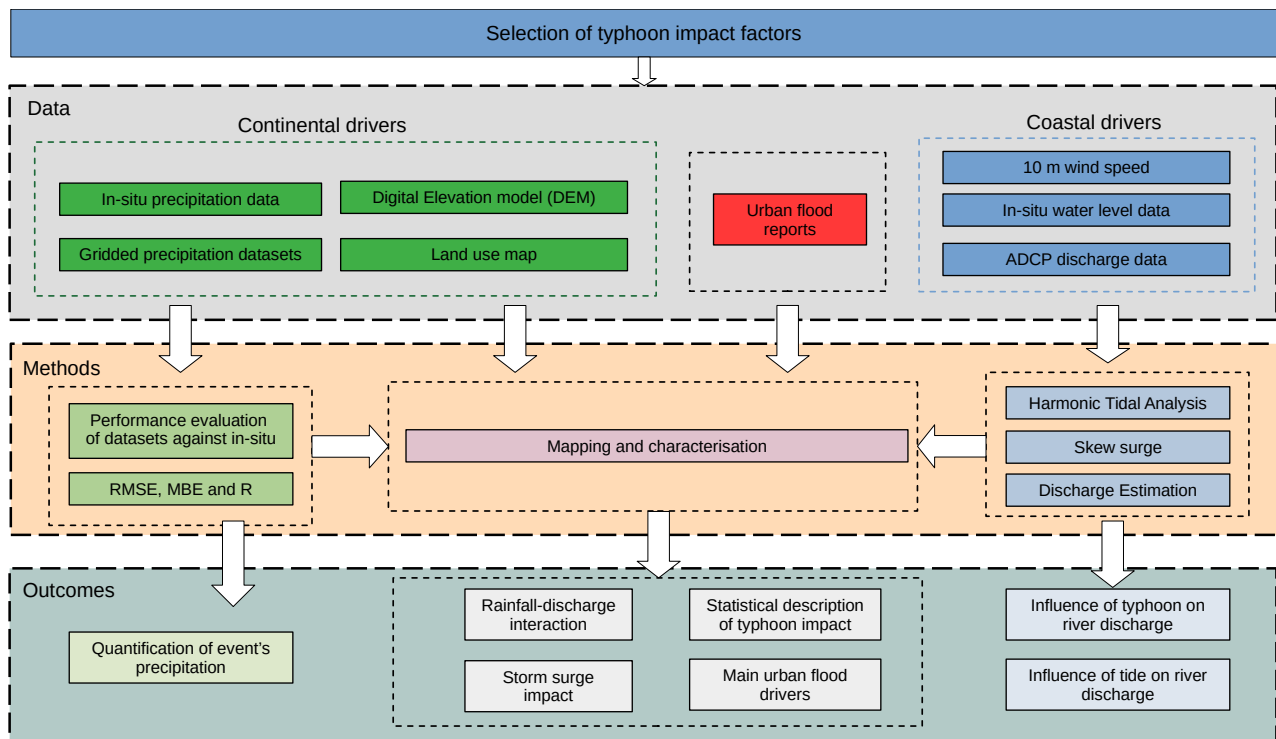
Figure 3. Framework to characterize and study the impact drivers of typhoon Usagi on the hydrological system.

In order to characterize the hydrological impact of TY Usagi on the tidal river system, the following general steps are applied (Fig. 3) and explained in detail in the following sections. We start by selecting a collection of data representative of the factors

influencing the impact of a typhoon. Different gridded precipitation products are evaluated against in-situ measurements to enable a high temporal and spatial resolution study of the precipitation pattern during Usagi. We study topography and land

100 use maps together with the obtained precipitation time series. Additionally, urban flood reports are mapped and analysed in order to form a holistic overview of the hydrological dynamics before, during and after the event. Lastly, we process in-situ water level measurements using harmonic analysis to obtain the astronomical tide and the residual water level. Furthermore, the skew surge is computed in order to quantify the storm surge effect. Finally, these signals are used to estimate the discharge of the river Saigon throughout the event.

105 ## 3.1 Performance evaluation of gridded datasets of precipitation over HCMC

The accuracy of 5 gridded satellite precipitation datasets was evaluated against in-situ measurements. In order to match the location of observations and dataset pixels, the precipitation values of the datasets were spatially interpolated to the location of ground observations using the bi-linear interpolation method (Gaborit et al., 2013; Ang et al., 2022). Additionally, we match the temporal resolution of the datasets and the observations such that a evaluation can be made. We chose the cumulative

110 precipitation over 3 days as the adequate time resolution for the period of available observed precipitation data (2016-2018). The evaluation was performed over 9 rain gauge locations where the data quality and availability of ground observations were deemed sufficient. The evaluation was carried out using three statistical indicators: mean bias error (MBE), root mean square error (RMSE) and correlation coefficient (R). These indicators have been widely used in literature for this purpose (Xiang et al., 2021; Ang et al., 2022). MBE is a statistical assessment of the mean difference between the interpolated and observed

115 rainfall, and RMSE represents the standard deviation between the dataset and the observations. The lower absolute values of MBE and RMSE indicate the better performance of the gridded dataset. R measures the degree of linear correlation between the gridded and observed datasets. Higher values of R indicate higher accuracy of the product in estimating precipitation. The equation, range, and optimal value of each index are presented in Table 1.

Table 1. Equations and optimal values of statistical indices. P_i and O_i denote predicted and observed values, respectively, of precipitation on the ith day.

Indices	Equation	Range	Optimal values
Mean Bias Error	$MBE = \frac{1}{N}\sum_{i=1}^{N}(P_i - O_i)$	$-\infty$ to ∞	0
Root Mean Square Error	$RMSE = \sqrt{\frac{1}{N}\sum_{i=1}^{N}(P_i - O_i)^2}$	0 to ∞	0
Correlation Coefficient	$R = \frac{cov(P,O)}{s_P s_O}$	-1 to 1	1

3.2 Ground-based and satellite precipitation datasets

120 Table 2 summarizes the precipitation datasets and observations used in this study. Gridded precipitation products can be classified into three categories based on differences in the data sources and retrieval models including gauge-interpolated, satellite-based, and reanalysis precipitation datasets (Jiang et al., 2021). Satellite-based datasets use polar-orbiting passive microwave

Table 2. Overview of the precipitation data used in this study. The categories are indicated as follows: gauge-based data (G), satellite-based data (S), reanalysis data (R) and in-situ data.

Name	Variable	Category	Temporal/Spatial Resolution	Temporal Coverage	Reference
GPCC	Rainfall	G	Daily/1.0°	1982-2019	Ziese et al. (2020)
CMORPH v1.0	Rainfall	S	3-hourly/0.25°	1998-2021	Joyce et al. (2004)
MSWEP v2.0	Rainfall	G, S, R	3-hourly/0.25°	1979-2021	Beck et al. (2019b)
ERA5	Rainfall	R	Hourly/0.5°	1979-2021	Munoz-Sabater et al. (2021)
IMERG	Rainfall	S	3-hourly/0.1°	2000-2021	Huffman et al. (2019)
Urban rain gauges	Rainfall	in-situ	daily/N.A.	2016-2018	HCMUDC - HOS

(PMW) sensors on low-Earth-orbiting satellites and geosynchronous infrared (IR) sensors on geostationary satellites to estimate precipitation (Larson and Peck, 1974; Kidd and Huffman, 2011). Often this datasets offset their limited abilities by
125 blending rain gauge data with their measurements (Mizukami and Smith, 2012). Reanalysis-related datasets generate several meteorological variables with a consistent spatial and temporal resolution by assimilating observations such as weather stations, satellites, ships, and buoys based on different climate models. In this analysis 5 datasets that belong to the three categories were chosen in order to examine their different performances over HCMC. All datasets that were used are freely available online via public repositories.

130

Global Precipitation Climatology Centre (GPCC) dataset. The GPCC provides the largest gauge-based dataset product derived from quality controlled station data sourced from national meteorological and hydrological services, global and regional data collections as well as WMO GTS-data. This GPCC product is recommended to be used when the daily precipitation information is of highest importance, e.g. for analyses of extreme events and related statistics at daily resolution. Despite its low
135 spatial resolution, the GPCC product was chosen as the gauge-based dataset since it is recommended for analyses of extreme events and related statistics at daily resolution (Jiang et al., 2021).

Climate Prediction Center MORPHing technique (CMORPH) dataset. This product consists of satellite precipitation estimates that have been bias corrected and reprocessed using the CMORPH to form a global, high resolution precipitation analysis
140 at very high spatial and temporal resolution. We chose this product due to its advection scheme of cloud features and wide range of applications including hydrological studies and extreme event analysis (Joyce et al., 2004).

Multi-Source Weighted-Ensemble Precipitation (MSWEP). MSWEP is a global precipitation product which incorporates daily gauge observations and accounts for gauge reporting times to reduce temporal mismatches between satellite-reanalysis
145 estimates and gauge observations. It was chosen for the study because it merges gauge, satellite, and reanalysis data to obtain precipitation estimates. MSWEP has demonstrated higher overall accuracy than other widely used precipitation products in

both densely-gauged and ungauged regions (Beck et al., 2017, 2019a). Beck et al. (2019b) provides a detailed description of the MSWEP V2.2 methodology.

150 ***European Centre for Medium-Range Weather Forecasts (ECMWF) Re-Analysis product (ERA5).*** The ERA5 product is the fifth-generation atmospheric reanalysis to replace ERA-Interim produced by ECMWF. It assimilates observations from over 200 satellite instruments or types of conventional data and information on rain rate from ground-based radar-gauge composite observations. Even though ERA5 has shown stronger data deviations than in bias-corrected satellite-based precipitation datasets (Islam and Cartwright, 2020), it was chosen since it can capture the spatial distribution of typhoon precipitation centers (Jiang et al., 2021).

155

Integrated Multi-satellitE Retrievals for Global precipitation measurement (IMERG). The IMERG product combines information from the GPM satellite constellation to estimate precipitation over the majority of the Earth's surface. The product fuses the early precipitation estimates collected during the operation of the TRMM satellite (2000 - 2015) with more recent precipitation estimates collected during operation of the GPM satellite (2014 - present). IMERG was chosen given that it generally

160 shows high accuracy and good performance in hydrological simulations when compared with the ground observations (Ang et al., 2022) as well as its good capability in extreme rainfall events applications (Huang et al., 2019).

Rain Gauge observations. We use daily rainfall data from nine rain gauges located in and around the city center of HCMC

165 as shown in Figures 1a) and 1b). This data was provided by the Ho Chi Minh Urban Drainage Company (HCMUDC) and the Hydrometeorological Observatory - Southern region (HOS) for the period from May 1st, 2016 to November 30th, 2018.

Table 3. Overview of water level, flood reports, topography and land use data used in this study. The categories are indicated as follows: gauge-based data (G), satellite-based data (S), reanalysis data (R) and in-situ data.

Name	Variable	Category	Temporal/Spatial Resolution	Temporal Coverage	Reference
ERA5	10 m wind	R	hourly/0.25°	22-27/11/2018	Hersbach et al. (2020)
Tide gauge	Sea level	in-situ	daily/N.A.	2007-2021	Caldwell et al. (2015)
Urban river gauge	Water level	in-situ	10 min/N.A.	2017-2018	Camenen et al. (2021)
Flood reports	Location and flood depth	report	N.A./N.A.	25/11/2018	SCFC
Flood reports 2	Location	report	N.A./N.A.	25/11/2018	Leitold et al. (2021)
SRTM DEM	Elevation	S	N.A./90 m	N.A.	Farr et al. (2007)
Land Use	Land use	S	Yearly/30 m	2018	Phan et al. (2021)

3.3 Harmonic Tidal Analysis

The Saigon river discharge is highly influenced by the mixed, semi-diurnal tidal cycle and presents a relatively low net discharge (Nguyen et al., 2019b, 2020; Camenen et al., 2021). The water level time series are highly influenced by the tidal signal making it difficult to access the impact of typhoon Usagi on water levels. It is thus important to process and filter out the tidal component from observed time series. According to Cid et al. (2017), we first remove the average water level variability from the water level time series by subtracting the monthly moving average. Then, we follow the methodology proposed by Pugh and Woodworth (2012) to produce the tidal signal via classical harmonic analysis to extract information on the amplitude and phase of the tidal constituents. Classical harmonic analysis has been developed and widely used to analyze and predict tides (Jin et al., 2018; Trinh et al., 2020; Couasnon et al., 2022). The UTide package developed by Codiga (2011) and implemented in Python by Bowman (2020) was used for extracting the tidal constituents. This package provides harmonic analysis with up to 146 tidal constituents. We use all available constituents for our tidal prediction. However, we exclude the constituents whose harmonic constants usually include mostly quasi-periodic meteorological effects (Mm, MSf, Mf, Sa, Ssa, S1). Excluding these long-term constituents from the analysis avoids over fitting the tidal prediction with frequencies that capture non-astronomical effects on water level such as wind, temperature and atmospheric pressure (Parker, 2007). Additionally, the upstream location of some of the sensors justifies the use of constituents produced by nonlinear mechanisms in shallow water. These mechanisms alter the characteristics of the tidal waves and may include the effect of bottom friction, standing wave generation or local resonances due to interaction with varying topography (Pugh, 2004).

In order to obtain the non-tidal effects on water level we compute the difference between the observed water level and the predicted tide, i.e. the residual signal (see Fig. 7).

3.4 Skew Surge

The residual signal at the sea level gauge of Vung Tau (Fig. 1a) presents sporadic peaks and troughs due to small shifts in tidal phase. This is a common challenge in tide prediction analysis in systems with large tidal amplitudes which is the case here (Williams et al., 2016; Calafat and Marcos, 2020; Couasnon et al., 2022). Hence, in addition to the residual signal, we look at the skew surge which represents the excess water level over the high tide. This metric has seen relevant application in several coastal flooding studies (Williams et al., 2016; Haigh et al., 2016; Couasnon et al., 2022).

3.5 Water level data

Time series data at 10 minute intervals were obtained from a 2-year measurement campaign (2017-2018) directed by the Centre Asiatique de Recherche sur l'Eau (CARE). Measurements were performed using CTD Diver sensors at two locations: Phu Cuong and Thao Dien as shown in Figure 1. Phu Cuong and Thao Dien are located at about 137 and 60 km from the coast (along river), respectively. In Camenen et al. (2021) the quality of these measurements has been validated against data of the Center of Environmental Monitoring (CEM) of Vietnam. This data is complemented by the record at the Vung Tau tide gauge from the research quality dataset available through the Joint Archive for Sea Level of the NOAA National Centers

for Environmental Information (Caldwell et al., 2015). A statistical description of these datasets can be found on Table B1 in
Appendix B. The stations of Phu Cuong, Thao Dien and Vung Tau depicted in orange in Fig. 1 will also be referred to as the
upstream, urban and coastal stations, respectively.

3.6 Water Discharge Estimation

The instantaneous water discharge was estimated by applying a stage-fall-discharge (SFD) rating curve adapted from the
general Manning-Strickler law (Eq. 1), previously tested and validated by Camenen et al. (2017) and used to predict the total
discharge of the Saigon river in Camenen et al. (2021):

$$Q(t) = sign(S) \cdot K \cdot A_w(t) \cdot R_h(t)^{2/3} \cdot \sqrt{|S(t + \Delta t)|}, \tag{1}$$

with Q the water discharge [$m^3 s^{-1}$], $K = 27.06 \ m^{1/3}s^{-1}$ the Manning-Strickler coefficient , $R_h = A_w/P_w$ the hydraulic
radius [m], A_w the wet section [m^2], P_w the wet perimeter [m]. Note that A_w and P_w are both a function of the water level
and thus, of time. The term $sign(S)$ is equal to the sign of the slope, S, taking the values of +1 or -1. The energy slope, S [-],
is assumed equal to the water slope and is computed as:

$$S = \frac{H_{up} - H_{dn} + dH}{L}, \tag{2}$$

with the water level H_{up} and H_{dn} measured at Phu Cuong (PC) and Thao Dien (TD), respectively, and L the distance
between the two locations. Two additional terms are used in this model: dH and Δt. The former is used to compensate the
fact that the reference points of each location are different and unknown. The latter is a time lag required to account for the
propagation of the tidal wave between one location to the other. The values used in this study were $dH = -0.149$ m and
$\Delta t = -2$ h. The full observed water levels at Phu Cuong and Thao Dien were used to compute the total discharge of the Saigon
river. The predicted tidal signals obtained via harmonic tidal analysis at these stations were used to compute the discharge due
solely to tidal fluctuations. Then, the tidal discharge is subtracted from the total discharge in order to obtain a residual discharge
- the discharge due to non-tidal effects.

In Camenen et al. (2021), the model calibration is done using two ADCP campaigns: i. March 2017 during an asymmetric
tide and ii. September 2016 during a symmetric tide. During the asymmetric tide the equation has much more difficulty
following the discharge measurements than during the symmetric tide. The parameters K, dt and dz are calibrated one at a
time to optimize the Root Mean Square Error (RMSE). This provided good results (see Fig. A.11 in Camenen et al. (2021)).
However, in this study we improve this calibration by using a non-linear least squares fitting technique (not presented here).
This calibration method yielded better results for the estimation of discharge than in Camenen et al. (2021). We improve the
RMSE of total discharge during an asymmetric tide from 350 $m^3 s^{-1}$ to 185 $m^3 s^{-1}$ using K = 27 $m^{1/3}s^{-1}$, dt = 2.00 h and dz
= -0.15 m. Additionally, statistical information about the estimated discharge can be found in Table B3 in Appendix B.

A shortcoming of this model arises when analysing the estimation of discharge solely based on the tidal prediction. As
230 seen in Table B3, the mean tidal discharge is positive (60.17 and 66.73 m^3/s for the wet and dry seasons, respectively)
implying an overestimation of discharge. Several possible sources of error can be identified such as over sensitivity to the water
level measurement error and difficulty in capturing asymmetrical tide dynamics. Therefore, interpretation of these discharge
estimations must be made carefully. It is also important to note that a quasi-simultaneous increase in water level on both stations
leads to small changes in slope and thus, a small change in estimation of residual discharge. This factor is specially relevant
235 for large scale events that can affect the two water level measuring stations at the same time.

3.7 Other data

Topography. The topography maps were obtained from the NASA Shuttle Radar Topographic Mission (SRTM) 90 m DEM
Digital Elevation Database. The SRTM mission has provided digital elevation data (DEMs) for over 80 % of the globe. This
data is currently distributed free of charge by USGS and is available for download from the National Map Seamless Data
240 Distribution System, or the USGS ftp site. The vertical error of the DEM's is reported to be less than 16m (Farr et al., 2007).

Land Use. The land use map of the region around HCMC was obtained from the Large-scale Land Use Land Cover (LULC)
website (https://www.eorc.jaxa.jp/ALOS/en/dataset/lulc/lulc_vnm_v2109_e.htm). LULC information was derived using a random-
forest-based algorithm and several geospatial data sources, including Landsat and Sentinel-1 and -2 imagery (Phan et al., 2021).
245 The final product contains annual land cover information from 1990 to 2020 in Vietnam at a 30 m resolution. This data is in-
dependently validated with field surveys and visual interpretation data. The overall accuracy of the level-1 layer ranges from
86 % to 9 2%.

Wind. ERA5 outputs for 10 m u and v wind components were used to map the approach of typhoon Usagi towards the southern
250 coast of Vietnam. This data is provided free of charge at the Copernicus Climate Data Store (https://cds.climate.copernicus.eu)
with an hourly resolution and global grid of 0.25° for the period 1959 to present (Hersbach et al., 2020).

Flood data. Urban flood reports for November 25th, 2018 were provide by the DECIDER project (https://www.decider-
project.org) and originally obtained from the former Steering Center for Flood Control (SCFC) in HCMC. These include
255 coordinates of flooded streets and corresponding flood height. Additionally, a flood map based on manufacturing firms' reports
was obtained from Leitold et al. (2021).

4 Results and Discussion

4.1 Assessment of precipitation products

The results of all statistical indices (RMSE, MBE and R) for each station are presented in Fig. 4. The worst performing dataset
over this domain is ERA5 with large values of RMSE and MBE (both > 100 mm/3 days) and low linear correlation (R ≤ 0.4).
This indicates that ERA5 is overestimating rainfall over the whole domain. The ERA5 dataset that was evaluated has a 0.5°
grid which is not capable of capturing the precipitation patterns over HCMC. The other gridded products perform relatively
well in stations within the city center (20 ≤ RMSE < 50; -20 ≤ MBE < 50 mm/3 days). This indicates that all datasets,
with the exception of ERA5, are able to estimate rainfall patterns over HCMC. The gauge-based dataset GPCC is able to
do so with the most coerce grid: a daily temporal window and spatial resolution of 1°. Even though CMORPH presents a
sophisticated advection scheme (0.25°), its performance is similar to the higher spatial resolution IMERG (0.1°) across all
metrics. Additionally, the performance of MSWEP (0.25°) is slightly better than CMORPH over the city center. However, this
better performance can also be attributed to the incorporation of in-situ data in addition to the satellite data used to produce
MSWEP. Nonetheless, this shows that a grid size of 0.25° suffices to estimate rainfall over HCMC using hybrid measurements
sourced from satellites and in-situ data.

The degree of linear correlation between all datasets and rainfall gauges is always below 0.7 for almost all stations. MSWEP
shows higher values of R (0.4 ≤ R < 0.7) than all other datasets. In fact, all other datasets show very low values of R (R <
0.5) indicating that these datasets have a weak linear relationship with the observed daily data. The main factor contributing to
the difficulty in accurately portraying the precipitation over Ho Chi Minh City is the convective pattern of precipitation events
leading to the non-uniform distribution of rain at the scale of the city (Vachaud et al., 2019). It can happen that it rains heavily
in one district whereas in another it does not rain at all. The spatial resolution of all datasets (always at least ≥0.1°) remains
too coarse to accurately capture the spatial variability during rainfall events. Additionally, this evaluation is undertaken at the
relatively high timescale of the day against scarce insitu measurements (both in time and space) which impacts the performance
of the datasets.
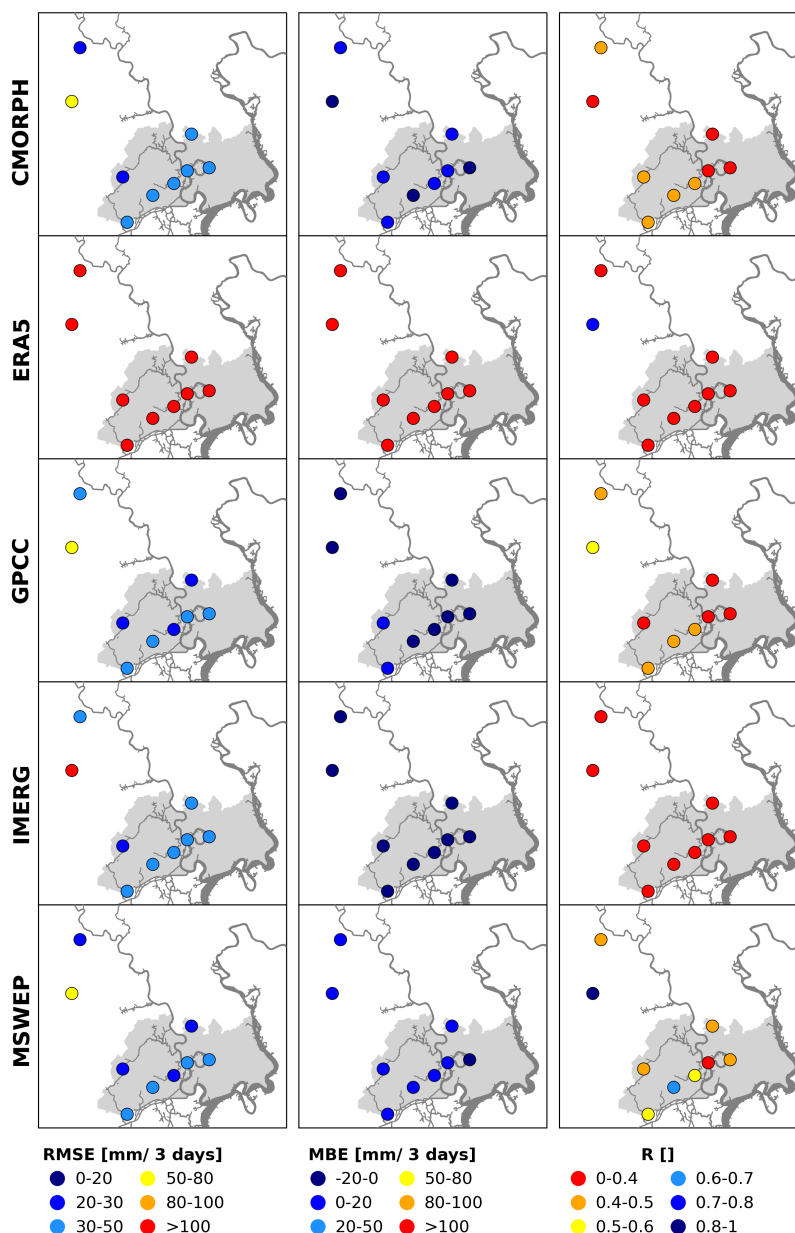
Figure 4. Spatial distribution of root mean square error (left), mean bias error (middle) and correlation coefficient (right) between 5 gridded products and gauged observations at daily time scale during 2015-2018. The circles denote rainfall gauging stations located in and around the Ho Chi Minh City (HCMC) area (light grey). The Saigon-Dong Nai system is represented in dark grey.

Overall, MSWEP is the dataset that better represents the precipitation patterns over HCMC by either showing similar metrics or outperforming other datasets especially in coefficient of correlation, R. In order to further validate this dataset, the performance metrics (RMSE, MBE and R) were computed for the moth of November 2018 on a daily timestep. In Fig. 5 the

precipitation products are plotted against the available rain gauge data (in grey bars). The extreme rainfall brought by typhoon Usagi on November 25th, 2018 is clearly seen in both rainfall gauge and datasets. For this period the rain gauge data is scarce with 3 out of 9 stations not having any measurements namely, Pham Van Coi, Thanh Da and Cau Bong. Additionally, the stations that present measurements have important data gaps. All datasets to the exception of ERA5 underestimate rainfall during Usagi. ERA5 (brown curve in Fig. 5) overestimates it with values above 500 mm for the day that Usagi made landfall. However, for the presented rainfall gauge measurements MSWEP (in light blue) seems to capture the precipitation behaviour during typhoon Usagi better than all other datasets (Table A1 in Appendix A). For MSWEP, the average statistics over the month of November 2018 and over all stations for RMSE, MBE and R are 7.6 mm/day, -4.3 mm/day and 0.6, respectively.
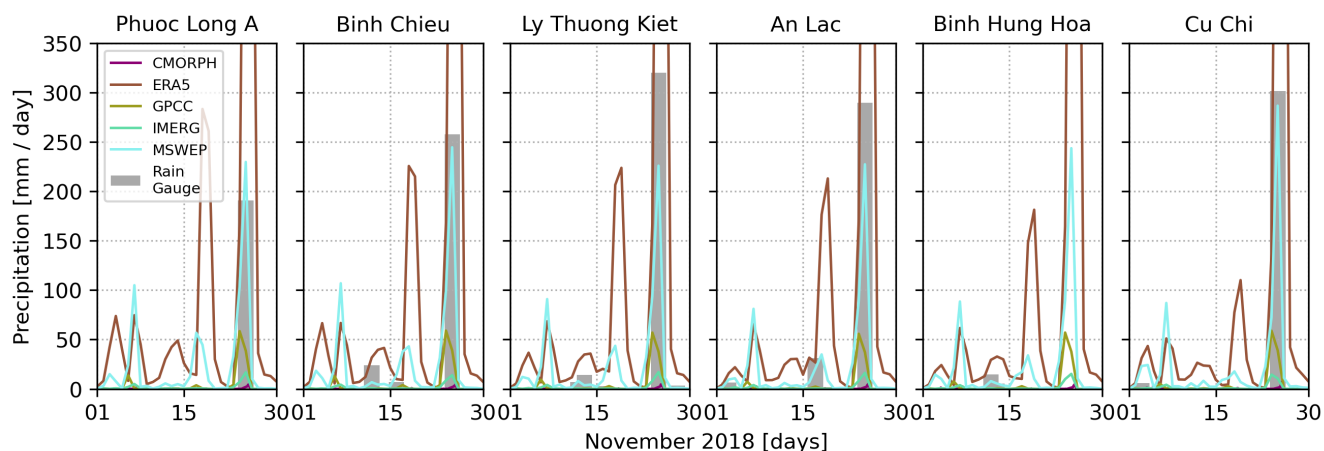
Figure 5. The 5 precipitation products compared to the 6 rain gauges with available observations for the month of November 2018. The peak of precipitation during typhoon Usagi is best captured by MSWEP (light blue) whereas the other datasets either underestimate or overestimate it. The ERA5 (brown) presents estimations above 500 mm. The high spatial variability over the city makes it hard to obtain accurate results at all stations simultaneously.

4.2 Statistical analysis of data and characterisation of TY Usagi

In this section we perform a seasonal statistical overview of water level, discharge and precipitation. Additionally, we quantify the effect of TY Usagi on these hydrological variables in comparison to seasonal variations. The boxplots referring to this data are presented in Fig. 6. The x-axis for the water levels are separated into the direct measurement (referred to as "Observed"), the tidal signal predicted via harmonic tidal analysis ("Tidal"), the signal without tidal influence ("Residual") and the computed skew surge ("Skew surge"). Similarly, for the discharge computed at Phu Cuong the estimations are divided into "Observed", "Tidal" and "Residual".

4.2.1 Seasonal patterns

Predicted tide: As can be see in Figures 6(a), 6(b) and 6(c), the predicted tide signal presents no seasonality as its average,
300 median and interquartile range do not vary between wet and dry season. However, the tidal signal changes from Vung Tau
at the coast towards upstream at Phu Cuong in the river Saigon. The whiskers in the boxplots decrease in size from coast to
upstream which means tidal amplitude decreases. We verify a decreasing tidal amplitude from 3.9 m (4 m) at the coast, to 3.1
m (3.2 m) at the urban city center, and to 2.7 m (2.5 m) upstream during wet (dry) season. This is equivalent to a decrease in
tidal amplitude of 8 mm per along river km between the coast and the city center and of 11 mm per along river km between
305 the city center and upstream of HCMC. It can also be seen that negative water levels can reach greater values in modulus than
positive water levels. This is due to the very low low tides during spring tidal cycles, as illustrated in Fig. 7(a). Additionally,
the size of the boxes decreases upstream which indicates the data is less spread in the river than at the coast, as the interquartile
range (IQR) is smaller. Furthermore, the box is closer to the higher values of water level at all stations. Hence, the probability
density function of the tide is skewed towards higher values. This is due to the asymmetric nature of the tide with cycles where
310 low tide is little pronounced and the lowest water level differs by less than 1 m from the neighbouring high tides (see Fig. 7a).

Observed water levels: The observed water level signals show average water levels that are higher than the tide prediction
during the dry season and lower during the wet season. This behaviour is counter intuitive from an hydrological point of view
where water levels are strongly connected to seasonal rains. This seasonality pattern in the coastal water levels is in line with
Trinh et al. (2020) and it propagates upstream as shown in Camenen et al. (2021). This clarifies that river water levels are
315 interconnected to seasonal coastal storm surge caused by the wind pattern of the East Asian summer monsoon, typically from
November to April (Marchesiello et al., 2020). Thus, the monsoon wind overpasses precipitation effects on the Saigon river.

Residual water levels and skew surge: For both seasons we expect the same behaviour as the observed time series and thus,
higher average residuals in dry season than in wet season. The difference on average residual between seasons is of 24 cm at
the coast, 26 cm at the urban center and 18 cm at the upstream station. As for the seasonal difference of average skew surge we
320 find 19 cm at the coast, 23 cm at the urban center and 17 cm at the upstream station. These results show that at the urban center
we have consistently higher surges than at the coast or than upstream which indicates that the surrounding highly urbanized
land cover and complex canal system are playing a role in the water levels at this location. Additionally, both residual signals
and skew surge take on more negative values in the wet season as all values below the upper quartile (Q3) are negative. The
inverse is seen for the dry season as all values above the first quartile (Q1) are positive. This behaviour is due to the difference
325 in tidal and observed water levels. Observed water levels are lower than predicted in the wet season leading to negative average
residuals and skew surge and vice-versa for the dry season. This further justifies a seasonal surge in the river due to a seasonal
surge at the coast.

Discharge: The estimated discharge boxplots (Fig. 6d) show similar discharge due to tides during both seasons. However,
the observed discharge differs from wet to dry season. The dry season tidal discharge is similar to the observed discharge on
330 average, median and IQR. However, the observed discharge signal presents longer whiskers and thus, higher discharge values
with observed discharge between -1604 and 2492 m^3s^{-1} versus -1500 and 1500 m^3s^{-1} for the tidal discharge. This means

that in the dry season tides are the main driver for discharge in the Saigon and less frequent but higher values occur due to other factors. Such factors include the outlier precipitation events during the dry season (see Fig. 6e). On the other hand, the wet season average and median discharge are respectively 168 and 217 m^3s^{-1} higher than for the tidal discharge. The larger

335 observed discharge in the wet season is could be attributed to the more intense rainfall during this period: the average wet season daily rainfall is 22 mm against 5 mm in the dry season averaged over the full watershed (Fig. 6e). As a result, the average residual discharge in the wet season is larger and the distribution is more spread (larger IQR) than in the dry season. This translates to an average residual discharge of 180 m^3s^{-1} in the wet season and 72 m^3s^{-1} in the dry season.
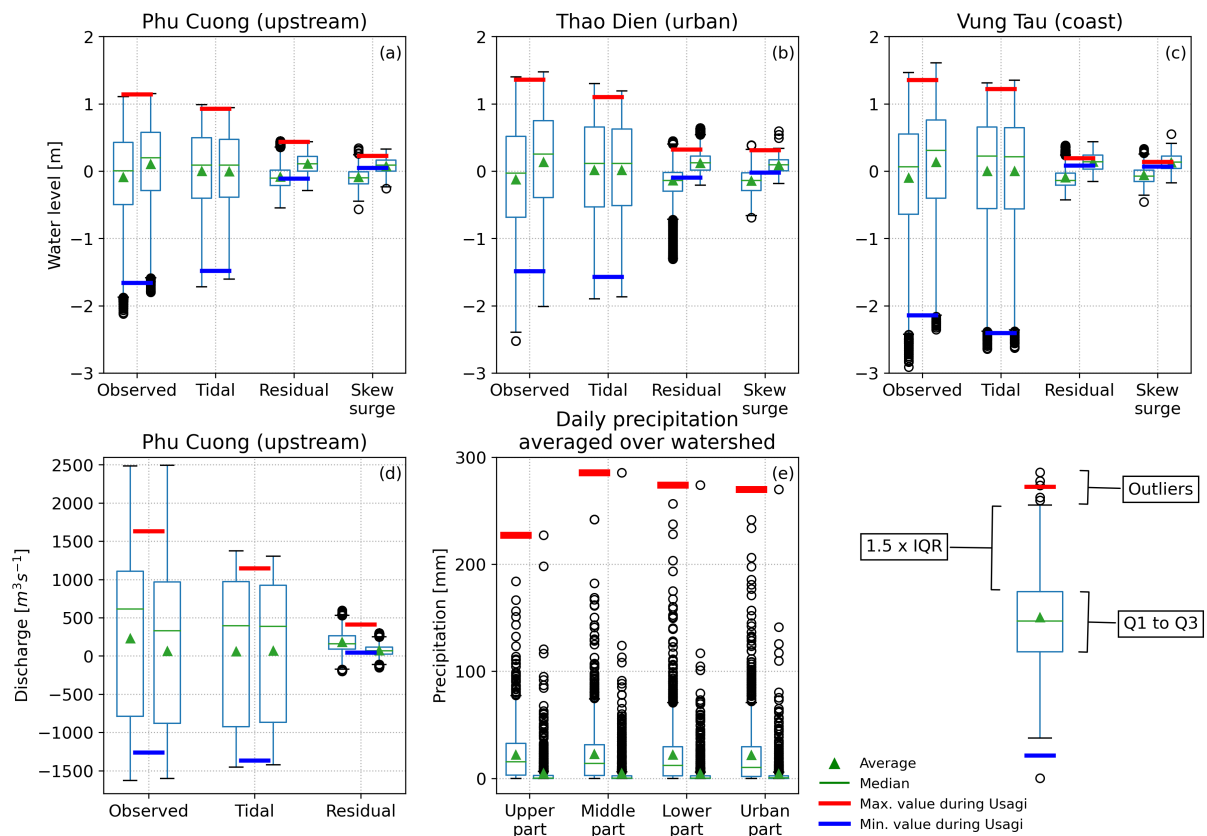
Figure 6. Boxplots of water level (observed signal, tidal prediction, residual signal and skew surge) for the upstream station of Phu Cuong (a), the urban station of Thao Dien (b) and the coastal station of Vung Tau (c). Boxplots of estimated discharge (using observed water level signals, tidal prediction and residual signals) for Phu Cuong (d). Boxplots of daily cumulative precipitation averaged over the spatial extent of the upper, middle, lower and urban parts of the watershed (e). Each variable in the x-axis has two boxplots corresponding to wet (left) and dry (right) seasons. A legend of the boxplots is provided in the bottom right corner: the box extends from the first quartile (Q1) to the third quartile (Q3) and the whiskers extend from the box by 1.5 times the interquartile range (IQR = Q3 - Q1). Extreme values for TY Usagi are reported in red (max) and blue (min) horizontal bars and correspond to the time window from 24-11-2018 to 26-11-2018. The time period of the data presented here correspond to the temporal coverage in Tables 2 and 3.

Rainfall: In Fig. 6(e), it can be seen a clear increase of rainfall from dry to wet season over the whole watershed as expected.

340   We see a lot of outlier events in both seasons with the dry season sometimes having exceptionally high rainfall events that are well above the average even for the more rainy wet season. The increased wet season rainfall seems to not change the water levels at the seasonal time scale. This is because we have a clear increase in rainfall in the wet season but a decrease in water levels over the two river stations. This shows that coastal water level is the main driver of river water levels and not rainfall. On the other hand, we see a slight increase in discharge during the wet season. Several arguments could hold: firstly, the average

345   water levels decrease due to coastal influence but the slope of the river is not influenced and we still capture seasonal differences in discharge given that our discharge estimate is a direct function of river slope. This increased discharge is most likely lead by continental rainfall - runoff given that the upstream dam management decreases its outflow during the wet season and increases it in dry season to combat saline intrusion (Ngoc et al., 2014).

4.2.2   Effect of Typhoon Usagi (24-26 November, 2018)

350   **Water levels:** From Fig. 6(c), it can be seen that TY Usagi occurred during a large amplitude spring tide (see also Fig. 7) with a low tide below Q1 of the tidal levels at the coast. At this location both residual water level and skew surge are within the IQR for the dry season. Hence, one can infer that the storm surge at the coast was not statistically significant when compared with the distribution of values during this season. Furthermore, the maximum coastal residual water level and skew surge were of 19 cm and 14 cm, respectively, which corresponds to 5 cm and 1 cm above the respective dry season averages. At the urban

355   city center (Fig. 6b) skew surge is close to being an outlier with a value of 31 cm which is 22 cm above the seasonal average. The residual signal maximum would be an outlier in the wet season and in the dry season it is above Q3 with a value of 32 cm which is 20 cm above the seasonal average. Finally, at the upstream station skew surge due to Usagi is less statistically significant than at the city center with a value of 23 cm which is above Q3. However, the residual signal is stronger at this location than at the city center with a value of 44 cm and 33 cm above the seasonal average.

360   For the time scale of the event (3 days) we find a statistically significant river surge but not a coastal surge. Therefore, there was no impact of coastal water level surge and the river surge seems to be due solely to continental drivers such as rainfall. The Saigon river's water level seems to follow the seasonality of the sea level but at short time scales it is impacted by continental factors. This could be partly explained by the apparent lack of storm surge (see Sect. 4.3).

Discharge: The Usagi impact seems to have brought about higher discharge at the upstream location of Phu Cuong than

365   usual. The discharge peak sits well above Q3 for the wet season and is a clear outlier for the dry season. The peak discharge during Usagi was 413 m^3s^{-1} which corresponds to 233 m^3s^{-1} above the average of the wet season. It can also be seen that there have been higher discharges in the wet season during the period of this data even though it is clearly an outlier discharge for the dry season.

Rainfall: In Fig. 6e) it is confirmed that the rainfall brought by Usagi constituted the maximum daily rainfall in this data

370   series for both wet and dry seasons. On the day of the landfall (November 25th, 2018), it rained on average 227 mm over the upper part, 285 mm over the middle part, 274 mm over the lower part and 270 mm over the urban part of the watershed (see Fig. 1).

4.3 Coastal driver: Storm surge effect on river dynamics

The results from the harmonic tidal analysis are presented in Fig. 7 for the period of one month around the Usagi event.
375 Additionally, a statistical description of the residual water level signal can be found in Table B2 in Appendix B. The predicted
tide, shows a mixed semi-diurnal character for the three stations (Fig. 7b). The observed time series of water level (Fig. 7a)
illustrates how the tidal wave propagates from the coast at Vung Tau to the upstream river stations. The tidal forcing is dominant
along the river system even throughout the Usagi event where no direct impact can be observed on the water level timeseries.
This is expected (see Sect. 4.2) and further certifies that the Saigon river's hydrodynamics are mainly controlled by tidal
380 forcing.

Storm surge is produced by water being pushed onshore by the force of the winds moving cyclonically around the storm. The
impact on surge of the low pressure associated with intense storms is minimal in comparison to the water being forced toward
the shore by the wind (NOAA, 2023). Additionally, many other factors, such as angle of approach of the typhoon, radius of
maximum winds and the slope of the continental shelf may also have an influence (Sebastian et al., 2019). Storm size also
385 significantly contributes to the generation of storm surge (Trinh et al., 2020) and provides an indication of the spatial region
influenced by the typhoon. Larger typhoons create higher storm surges and coastal inundation (Orton et al., 2015). Therefore,
we use the wind field to determine wind direction and the size of the TY Usagi (Fig. 2).

A clear anomaly during the event can be seen when using the harmonic tidal analysis methodology to obtain a water level
without tidal influence (namely, the residual water level, Fig. 7c). Both river stations present an increase in water level after
390 landfall (Fig. 7c, black and grey lines). On the other hand, the coastal response is not evident (Fig. 7c, blue line). This indicates
that TY Usagi had a continental effect on the hydrological system rather than a coastal effect. Additionally, from the wind
vector maps of Fig. 2(b-d) it can be seen that offshore winds are created at the Vung Tau region due to the direction and angle
of approach of TY Usagi. Hence, throughout the event strong onshore winds never occurred which explains the lack of storm
surge at the coast (Fig. 2(a) and Fig. 7c). Examining the skew surge results of Fig. 7(d) further motivates a lack of coastal storm
395 surge but a significant river surge (as seen in Sect. 4.2) after landfall. Furthermore, the event reaches land coinciding with a
very low coastal water level during a spring tide (Fig. 7b). This result is in line with the study of (Takagi et al., 2014) which
modelled storm surge in Vietnam and found that the potential maximum of the storm surge for the southern sections is rather
low (0.7 m) due to the S-shape of the country's shoreline and the cyclonic rotation of typhoons in this region. The lack of storm
surge during TY Usagi is not unprecedented particularly along the Vietnam coast. Trinh et al. (2020) show that even some of
400 the strongest historical typhoons that hit Vietnam can show no record of high storm surges in certain locations along the coast
of Vietnam, namely near the cities of Da Nang and Quy Nhon. This indicates that more studies following the methodology of
this paper could be valuable if applied to other urban hydrological systems in Vietnam or elsewhere in South East Asia.

A substantial decrease in residual water level at the two river stations (Thao Dien and Phu Cuong) prior to landfall can also
be seen (Fig. 2a). This suggests that at the timescale of the event river and coastal water levels are decoupled: river stations
405 experience negative residual prior to landfall and a significant surge after landfall whereas the coastal station does not.
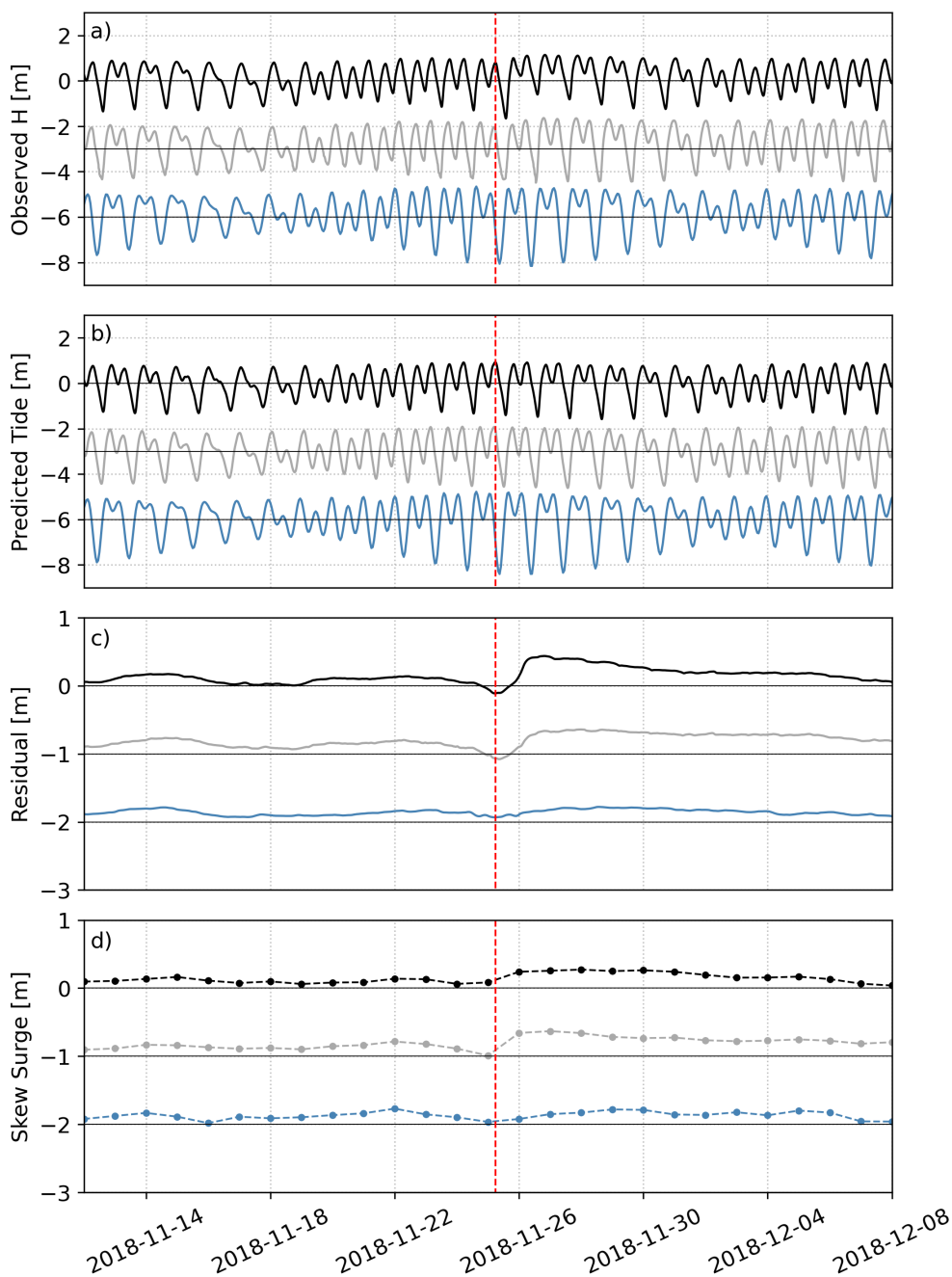
Figure 7. Result for tide prediction at the river stations - Phu Cuong (black) and Thao Dien (grey) - and the coastal station Vung Tau (blue). Timeseries of the full observed signal (a), the tidal prediction (b), the residual (c) obtained by subtracting the tidal prediction from the observed signal and the skew surge (d). For the sake of readability, the signals in (a) and (b) are displaced by 3 meters and the signlas (c) and (d) by 1 meter. Additionally, the vertical, red line represents the time of landfall of typhoon Usagi at Vung tau.

4.4 Continental driver: Rainfall effect on river dynamics

As seen in Sect. 4.2, TY Usagi brought heavy precipitation over the region. In order to better understand the effect of this event on river discharge we map the Saigon system, the topography of the region, the land cover and the spatial distribution of rainfall (Fig. 8a-f). The watershed, urban center and water level stations are also shown in Fig. 8(a).

410   The watershed is divided into four parts: the upper part (2538 km^2) around the Dau Tieng reservoir; the middle part (1840 km^2) which extends south from the reservoir, encompasses the first 80 km of the Saigon and crosses it about 2 km north of the Phu Cuong water level station; the lower part (548 km^2) extending down to the urban center and that encompasses 14 km of river and a complex canal network that flows into it; and, finally, the urban part (211 km^2) which encompasses the last, very sinuous 42 km of river, the urban canal network and the Thao Dien water level station. In the following, we assume that the
415   upper part of the watershed has no direct influence on the river Saigon.

The DEM (Fig. 8b) represents the flatness of the region with the middle, lower and urban parts of the watershed sitting well below 50 m amsl. Further, the lower and urban parts are mostly at an altitude below 10 m amsl (see Fig. 10a). In fact, the slope of the water surface between the upstream and urban water stations is of the order of 10^{-5}. The distance between these stations is 20 km in a straight line and 35 km along river.
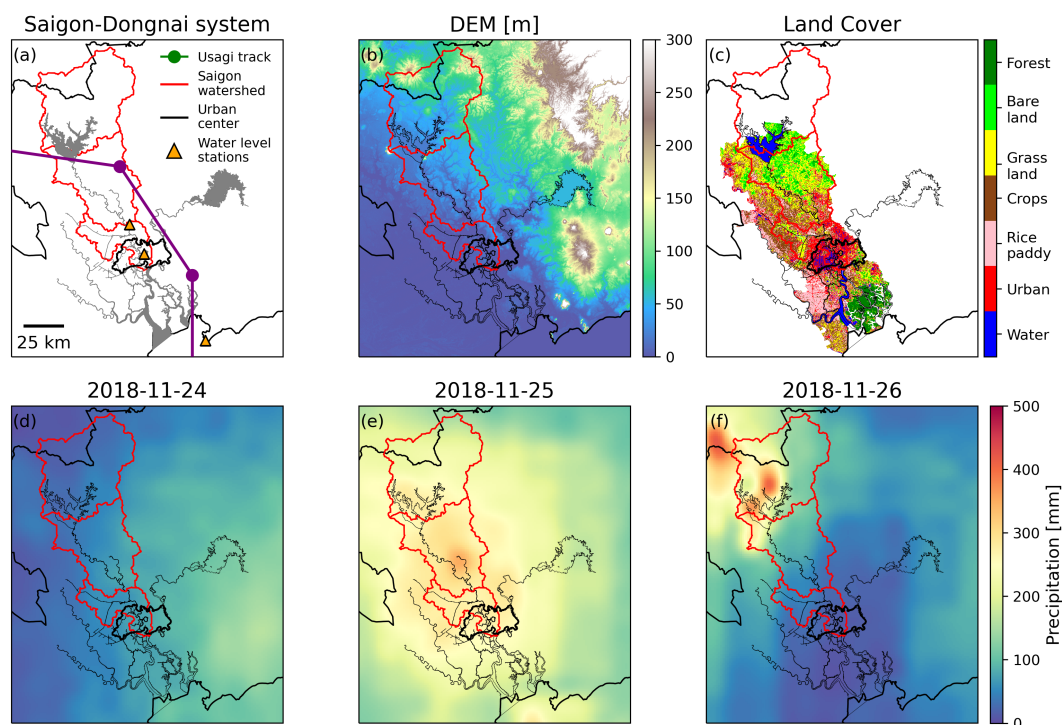
Figure 8. (a) The Saigon - Dongnai system, TY Usagi trajectory and the Saigon watershed. The watershed is split into 4 parts: upper, middle, lower and urban; (b) Digital Elevation Model (DEM) of the region; (c) Land use map of the region; (d-f) MSWEP daily precipitation over the three days of heavy precipitation connected to TY Usagi.

420   In terms of land cover (Fig. 8c) , the middle part of the watershed is composed of bare land and grass land in its northern half; of rice paddys, crops and grass land southwest of the Saigon; and of urban cover, crops and rice paddys southeast of the river. However, only about 15 % of this part is urbanized cover (Nguyen et al., 2022). The lower part of the watershed is mainly covered by crops and grass land west of the river and urbanized land to the east. The urban part is mainly urbanized land cover and waterways with the southeast corner with some grass land (see Fig. 10c).

425   In Fig. 8(d-f), the daily cumulative precipitation is plotted over the Saigon-Dongnai system. On November 24th, 2018 (the day before landfall, Fig. 8d) we see a spatially homogeneous precipitation over the whole watershed of about 100 mm. The following day Usagi made landfall at 06H UTC. Figure 8(e) shows that the bulk of the rainfall happened in the middle of the watershed with some locations with values above 300 mm. The lower and urban parts also witnessed heavy rainfall between 200 and 300 mm. On November 26th, 2018 Usagi was already over Cambodia. The bulk of the rainfall occurred on the upper

430   part of the watershed. The northern part of the middle part of the watershed saw levels of precipitation above 100 mm while the lower and urban parts saw values below 100 mm.

     The discharge results during the period of TY Usagi are presented in Fig. 9(a) and the MSWEP precipitation summed over the watershed in Fig. 9(b). Residual discharge starts increasing after landfall whereas the precipitation event starts about 1 day before landfall on Nov. 24th, 2018. Additionally, peak precipitation occurred 10 hours after landfall (16H UTC Nov. 25th,

435   2018) with a volume of 65 mm over 3 hours and peak discharge occurred about 26 hours after landfall (8H UTC Nov. 26th, 2018) and thus, with a time lag of 16 hours after peak precipitation. Considering that the middle part of the watershed is the main driver of residual discharge at Phu Cuong, this time lag can be partially explained by the very flat nature of the terrain (Fig. 8b). As shown in Fig. 8(c) , the middle part of the watershed has a significant amount of vegetation which intercepts precipitation and slows the movement of water into river channels.

440   Wide spread flooding could have played a role in delaying the discharge response. An analysis of flood areas was conducted using MODIS satellite daily and 8-daily surface reflectance products (Fig. A1 in Appendix C). This analysis proved difficult to interpret within the watershed area due to the presence of clouds throughout the event. However, we found evidence of widespread flooding immediately east of the watershed around the river Vam Co Dong which has similar land cover as the middle part of the watershed (Fig. 8c).

445   Another possible driver of the lag time between rainfall and discharge are aquifer recharging processes. In the middle part of the watershed the groundwater is more influenced by rainfall than by river recharge with shallow aquifers being predominantly recharged by heavy wet season rainfall events (Tu et al., 2022). The existence of a time lag between rainfall and discharge at this location after such heavy rainfall might be due to the recharge of the groundwater table functioning as a buffer. Additionally, monitored groundwater levels are generally above the Saigon river's water level creating an hydraulic gradient from the shallow

450   aquifers towards the river (Khai and Koontanakulvong, 2015; Tu et al., 2022). This possibly indicates a groundwater recharge phenomenon followed by a slow spill towards the river over the few days following the event.
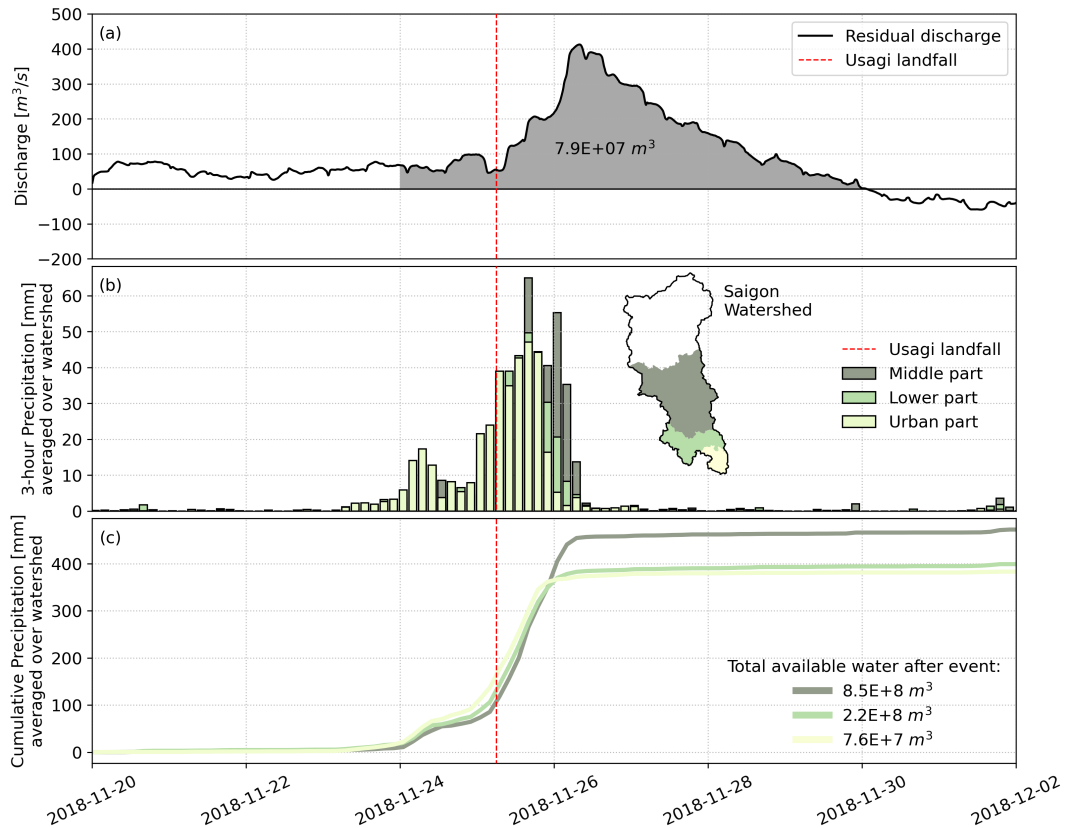
Figure 9. (a) Estimated residual discharge at Phu Cuong (upstream) and total volume output during TY Usagi; (b) MSWEP 3-hour precipitation averaged over the middle, lower and urban parts of the watershed. The upper part of the watershed is not considered since all runoff is directed towards the Dau Tieng reservoir. Additionally, the Saigon watershed is delineated in black; (c) MSWEP cumulative precipitation averaged over the middle, lower and urban part of the watershed as well as total available water after the event.

The residual discharge goes to zero about 41 hours after the precipitation event is over. During this time the Saigon river evacuated 7.9E+7 m³ of water at the Phu Cuong location where discharge is computed. On the other hand, the middle, lower and urban sub-catchments received a total of 472, 399 and 383 mm of cumulative rain (Fig. 9c). This equates to, respectively,
455   8.5E+8, 2.2E+8 and 7.6E+7 m³ of available water after the event. Assuming the middle part of the watershed is the principal driver of the residual discharge at Phu Cuong the river evacuated a 9.3 % of all available water. This low percentage of evacuation is partly explained by the important role that evapotranspiration plays in the climate of the region, which can effectively reduce the peak discharge of the river. Rujner and Goedecke (2016) use the water budget model ABIMO to describe the long-term annual means of the total run-off, surface run-off, evaporation and infiltration around HCMC. The results show
460   that surface runoff takes 7 %, infiltration 6 % and the remaining 87 % is evapotranspiration which is in line with our findings.

We can also see (Fig. 8f) that the upper part of the watershed received heavy precipitation on Nov. 26th, 2018. However, from Fig. 9(a) there is no discharge response of the Saigon river which justifies assuming that the upper part of the watershed

is not influencing the river's discharge. This part of the watershed is regulated by the Dau Tieng reservoir which is managed by Dau Tieng-Phuoc Hoa Irrigation Exploitation Company. According to its design, the maximum capacity of overflow discharge

465 is of 2800 m^3s^{-1}. However, during the dry season the maximum output from the dam is 30 m^3s^{-1} and during the wet season it is around 100 m^3s^{-1} with peaks that can go up to 400 m^3s^{-1} during heavy rainfall events (Dinh and Nguyen, 2019). The reservoir has only one available flood route which is the Saigon river. The flood capacity of the Saigon river section at the foot of the dam is much lower than the maximum overflow capacity causing severe downstream flooding every time the discharge through the spillway exceeds 200 m^3s^{-1}. Ever since 2013, the province of Ho Chi Minh City ensures that the reservoir flood

470 discharge capacity is kept below 500 m^3s^{-1}. However, when heavy rains are predicted the dam's discharge can be increased to levels close to the peak residual discharge found in Fig. 9. It is thus, possible that part of the residual discharge is a direct cause of the dam's discharge policies which would make the evacuation of rainfall by the river even smaller.

Even though a river response to rainfall is seen, the residual discharge provoked by the storm is negligible when compared to the total discharge amplitudes due to the tidal forcing (Fig. 6d). Hence, tidal forcing dictates the Saigon's dynamics even

475 during an unprecedented extreme rainfall event. Nonetheless, the behaviour of the residual discharge follows closely the water level's behaviour with a similar time lag in the hydraulic response (see Figures 9a) and 7c). This is expected as the driver of the discharge computation is the slope (Eq. 2) which is a function of the water levels at both stations. The relatively weak hydraulic response could be explained by the fact that both stations have a quasi-simultaneous increase in water level which leads to a less steep slope and thus, weaker discharge. Thus, a wide-spread precipitation event such as TY Usagi can cause increased

480 water level at both our measuring stations simultaneously making it hard to accurately use this model to estimate discharge.

4.5 Discussion

The greatest impact of TY Usagi on the population of the HCMC megalopolis came from urban flooding. In this section we discuss the flooding reports at the urban city center in connection with its topography, land use and rainfall extent.

As can be seen from Fig. 10(a), the HCMC is very flat (below 5 m amsl) with the highest part at the center with an altitude

485 of up to 15 m above msl. This higher topography is west of the urban watershed implying a surface runoff gradient from west to east into the Saigon river. The land cover is mainly impervious concrete (Fig. 10c) with some patches of grass land north of the city center.

In Fig. 10(d), the cumulative precipitation during TY Usagi can be found. We see an increasing South-North precipitation gradient which follows the direction of Usagi after it made landfall. The north of the city saw the highest amount of precipitation

490 (up to 400 mm) and the lower and urban parts of the watershed received between 350 and 370 mm. As seen in Sect. 4.4, this amounts to 8.4E+7 m^3 of available water after the 3 days of the event. By design, the proposed model to estimate discharge is not able to estimate discharge at the urban location. Hence, the direct evacuation by the river cannot be discussed. Nonetheless, the Thao Dien station showed a non-negligible increase in water level (see Sect. 4.2) pointing to a surface runoff effect. Rujner and Goedecke (2016) uses the ABIMO model to show that for the urban cover situation in 2016 the total runoff is 38 % of

495 the input by rain water. Thereafter the surface runoff has a share of 22 % and the infiltration 16 %. These values are indicative of the periodic urban flooding problems following heavy rainfall events in HCMC. For TY Usagi, these percentages translate

to 6.4E+6 m^3 of surface runoff and 4.6E+6 m^3 of infiltration over the urban part of the watershed. The values for total runoff (surface runoff and infiltration) represent 36.7 % of the total volume discharged (7.9E+7 m^3) at Phu Cuong after the event. This provides an indication that, contrarily to the upstream situation, the Saigon river might be capable of evacuating a substantial

500 amount of the rainfall within the few days after the event.

As reported by Vietnamese media, Thao Dien suffered heavy, prolonged flooding with some wards under water for over 24h. The spatial extent and depth of flooding can be found in Fig. 10(b). Indeed, the Thao Dien location shows the highest density of flood points but also the highest depths of flood (up to 0.8 m). Furthermore, flood depths of up to 0.4 m can be found in the highest elevations of the urban center namely, on the west of the urban watershed which in principle creates runoff in the

505 direction of the Saigon river and thus, towards the Thao Dien location.
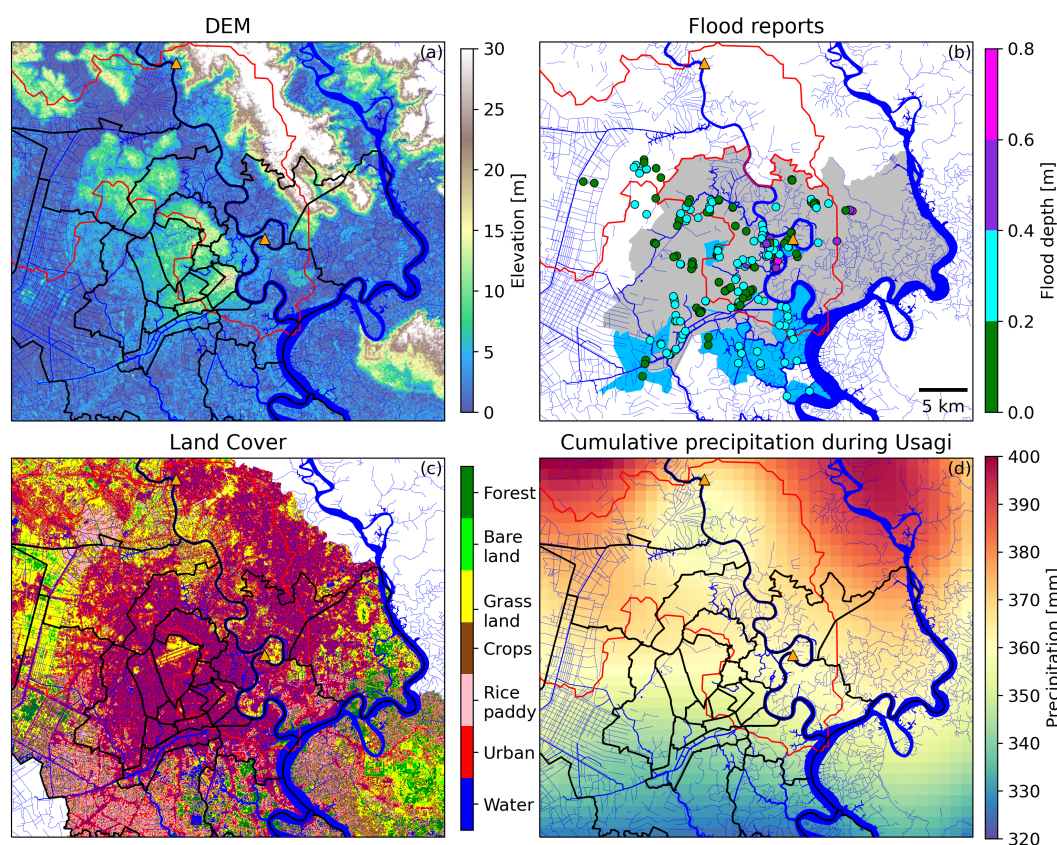
Figure 10. (a) Digital Elevation Model (DEM) of the urban city center. The Phu Cuong (upstream) and Thao Dien (urban) water level stations are indicated as orange triangles. The lower and urban parts of the Saigon watershed are delineated in red; (b) Flood extent and depth reported on November 25th, 2018; (c) Land use map of the urban city center; (d) Cumulative MSWEP precipitation during TY Usagi over the three days of heavy precipitation connected to TY Usagi (Nov. 24th-26th, 2018).

The observed time lag in water level increase at the Thao Dien station (Fig. 7c, grey) is compatible with the reported flooding locations and duration. Additionally, both peak rainfall and high tide (Figures 7(b) and 9b) coincided with the reported flooding duration. The high tide and heavy rainfall effectively removed the possibility of surface runoff to flow towards the river and flooding occurred around Thao Dien. This comes to show that despite the lack of storm surge at the fluvial-marine transition,
510   the coastal tidal forcing is still a main player in the dynamics of urban flooding in HCMC even during TY Usagi.

5   Conclusions

In this paper, we investigate the most severe rainfall event ever experienced in Ho Chi Minh City (HCMC), Vietnam. It occurred on November 25th, 2018 when typhoon Usagi directly hit HCMC. During this event, there was more than 300 mm of rainfall over 24h which led to flooding and considerable material damages. In this work, we put forward an evaluation of its impact on
515   the hydrological system of the region by using a set of tools to characterize and quantify both coastal and continental effects. For the first time in a data scarce region, all hydrological information was gathered and analyzed during an unprecedented extreme event that affected millions of people in the HCMC megalopolis. We go from an hydrological approach to a data analysis and signal processing approach in order to analyze coastal and river water levels, rainfall and flood. This approached not only allowed a thorough investigation of the typhoon's impacts but also allowed new insights on the hydrological behaviour
520   of this region.

From the evaluation of five research-quality precipitation datasets against in-situ measurements, we find that the MSWEP dataset shows the best performance in estimating rainfall over the region of interest and can capture the precipitation behaviour during TY Usagi ($R=0.6$; MBE=-4.3 mm and RMSE=7.6 mm). Hence, it is used to analyze TY Usagi's rainfall over the watershed. A statistical overview of the dataset shows that the rainfall brought by Usagi constituted the maximum daily rainfall
525   in the MSWEP data series.

We observe that the impact of increased wet season rainfall on river water levels is dwarfed by the seasonal coastal storm surge caused by the wind pattern of the East Asian summer monsoon, that typically lasts from November to April. This translates to higher water levels during dry season and thus, a coastal control of the Saigon river at the seasonal scale. A mono-disciplinary hydrologist approach may have expected a higher water level during the wet season, which underlines the interest
530   of crossing disciplines at the interface between river and ocean. Additionally, it was found that the highly urbanized land cover and complex urban canal system of HCMC are modulating the river water level which shows consistently higher residual water levels and skew surge than elsewhere.

The main coastal impact driver related to a typhoon event is the associated storm surge. At first, no direct observation of the hydrological impact of TY Usagi is possible on the Saigon river and harmonic tidal analysis was required to filter the
535   tidal fluctuations and observe the effects of such an event. For TY Usagi, the analysis of coastal residual water level and skew surge showed that the storm surge was not statistically significant when compared with the distribution of values during the wet season. The lack of coastal surge is associated with the timing of the landfall, the direction and the angle of approach of TY Usagi. Landfall occurred during a large amplitude spring tide with a very low tide and the typhoon never produced

strong onshore winds but instead offshore and shore-parallel winds. However, the lack of storm surge is mainly attributed to the wind direction during this event. On the other hand, the Saigon river's urban and upstream water level stations show a significant surge which shows that there was no impact of coastal surge on river water levels and that river surge was due solely to continental drivers such as rainfall. At short timescales and during the sudden, heavy precipitation event, the river and coastal water levels were decoupled.

After landfall, we find that both river levels and discharge start increasing whereas the precipitation event starts about 1 day before landfall. The peak precipitation and peak discharge occurred 10 and 26 hours after landfall, respectively. The very flat nature of the terrain in addition to the significant amount of vegetation create a time lag of 16 hours between peak discharge and peak precipitation. Furthermore, the river evacuates 9.3% of available rain water pointing to wide spread flooding and aquifer recharging processes in the middle of the watershed. In fact, the extreme rainfall brought about a peak discharge that is above the third quartile for the wet season but that is far from being an outlier. Even though, it was not possible to know the dam's discharge policy during Usagi it is clear that part of the residual discharge could be a direct cause of the dam's discharge. Historically, the dam's discharge policy was of increasing outflow in anticipation of heavy rainfall making the river contribution to evacuating of rainfall smaller.

The highest impact of this event takes the form of urban flooding with TY Usagi releasing 7.6E+7 m^3 of water over the urban watershed over 3 days. The urban water level station showed a non-negligible increase in water level pointing to a surface runoff effect. Our estimation says that urban total runoff is 36.7% of the water volume discharged at Phu Cuong and thus, at the urban location the river is able to evacuate the rain water over the few days after the event. Additionally, we find that the Thao Dien ward shows the highest density of flood points but also the highest depths of flood (up to 0.8 m). Furthermore, floods in the west of the urban watershed create runoff in the direction of the Saigon river and thus, towards the Thao Dien water level station explaining its consistently higher surges than in the upstream station. Time lag in water level surge and peak precipitation are due to the high tide removing the possibility of surface runoff to flow towards the river. This shows that despite the lack of storm surge the coastal tidal forcing is still a main player in the dynamics of urban flooding in HCMC even during TY Usagi.

The methodology presented in this paper encompasses a data processing and analysis work applied to a complex, urban estuarine system. Its foundation lies on the correct choice of typhoon impact factors and gathering of relevant, high-quality data in order to characterize the response of the hydrological system to an extreme event. This methodology could easily be applied to any other urbanized estuary both in South East Asia and elsewhere in the world by tailoring the choice of impact factors to the region of interest. Additionally, the extreme event need not be a typhoon but could be any other event that impacts the hydrological system and respective communities.

Future prospects would be high resolution modelling of the city's flooding regimes during typhoon events even though models of such complex hydrosystems have expected limitations. Additionally, simulating high numbers of typhoons around the area to find typhoon characteristics that would be more damaging to HCMC could be an interesting follow up. This would allow early warning depending on early developing storm characteristics and a better understanding of expected damages. Thus, providing the city with better information for impact mitigation. Finally, a better understanding of the upstream area of

HCMC and the interaction between river discharge, rainfall and groundwater is required as well as a better understanding of

575   the canal network dynamics.

Appendix A: Performance metrics for MSWEP during TY Usagi

Table A1. Performance metrics for MSWEP over the month of November 2018 over 6 rainfall gauges in HCMC.

Rainfall Gauge	RMSE[mm/day]	MBE [mm/day]	R [ ]
Phuoc Long A	7.2	20.2	0.62
Binh Chieu	4.2	-7.8	0.71
Ly Thuong Kiet	17.3	-20	0.8
An Lac	11.7	-15.8	0.77
Binh Hung Hoa	1.3	-3.5	0.11
Cu Chi	4.2	1.2	0.64
Average	7.6	-4.3	0.6

Appendix B: Statistical description of datasets

Table B1. Statistical description of water level data for the period from January 2017 to December 2018 at the three stations under study. The mean water level over the full period was removed from the series. All non-specified units are in meters.

Station	Vung Tau		Thao Dien		Phu Cuong	
Distance from coast	0 km		60 km		80 km	
Frequency	1 h		10 min		10 min	
Season	Dry	Wet	Dry	Wet	Dry	Wet
Count of data points	8224	8774	48312	52993	48312	52993
Mean	0.13	-0.01	0.14	-0.12	0.1	-0.09
Standard deviation	0.8	0.83	0.73	0.79	0.59	0.65
Minimum	-2.35	-2.91	-2.01	-2.52	-1.8	-2.12
25th percentile	-0.40	-0.64	-0.39	-0.69	-0.29	-0.5
50th percentile	0.31	0.07	0.26	-0.03	0.2	0.01
75th percentile	0.76	0.55	0.75	0.52	0.58	0.43
Maximum	1.61	1.47	1.48	1.4	1.15	1.11

Table B2. Statistical description of residual water level for the period from January 2017 to December 2018 at the three stations under study. All non-specified units are in meters.

Station	Vung Tau		Thao Dien		Phu Cuong	
Distance from Coast	0		60000		80000	
Season	Dry	Wet	Dry	Wet	Dry	Wet
Mean	0.14	0.02	0.12	-0.02	0.11	0.003
Standard deviation	0.16	0.21	0.16	0.25	0.17	0.21
Minimum	-0.33	-0.73	-0.75	-2.35	-0.46	-0.86
25th percentile	0.02	-0.14	0.01	-0.16	-0.01	-0.14
50th percentile	0.13	0.01	0.12	-0.003	0.1	-0.01
75th percentile	0.25	0.17	0.23	0.16	0.22	0.15
Maximum	0.76	0.76	0.91	0.94	0.93	0.93

Table B3. Statistical description of computed discharge for the period from January 2017 to December 2018 at Phu Cuong.

	Total Discharge [m^3/s]		Discharge due to tide [m^3/s]		Net Discharge [m^3/s]	
Season	Wet	Dry	Wet	Dry	Wet	Dry
Count	52993	48305	52993	48305	52993	46211
Mean	242.05	135.41	60.17	66.13	181.9	68.78
Standard Deviation	940.96	937.86	928.96	884.64	150.09	118.03
Minimum	-1626.45	-1513.89	-1454.15	-1421.38	-352.15	-535.28
25th Percentile	-777.9	-862.25	-924.57	-868.44	88.57	19.37
50th percentile	632.81	476.49	397.32	385.62	158.95	65.94
75th Percentile	1112.16	1042.00	970.93	923.61	267.18	117.24
Maximum	2482.67	1630.29	1376.30	1302.63	1769.07	987.94

Appendix C: MODIS satellite study
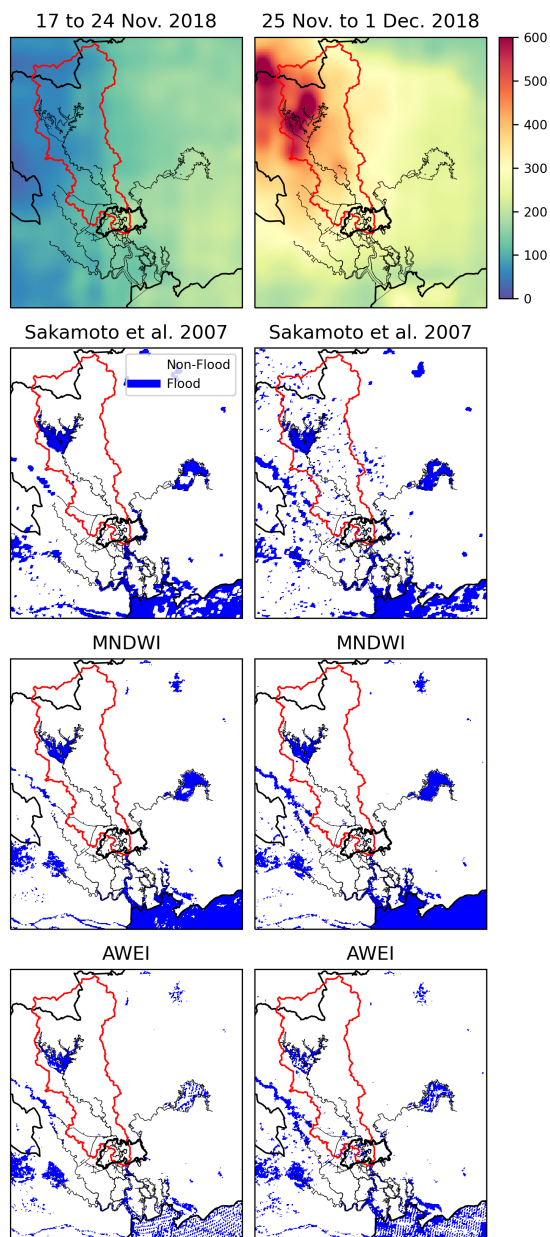
Figure A1. DEM, land cover, weekly cumulative precipitation and results of flooded area over the region of interest using MODIS surface reflectance 8-day product. The left column represents the week before the event and the right column the week after. Three methodologies are used to find inundated pixels: Sakamoto et al. (2007); Modified Normalized Difference Water Index (MNDWI); and Automated Water Extraction Index (AWEI).

Author contributions. Conceptualization, investigation, data collection and curation: Francisco Rodrigues do Amaral; Formal analysis, writing and editing: Francisco Rodrigues do Amaral; Reviewing and supervision: Nicolas Gratiot, Thierry Pellarin.

Competing interests. The authors declare having no competing interests.

Acknowledgements. We would like to thank to our colleagues at the DECIDER project and at the Centre Asiatique de Recherche sur l'Eau (CARE) laboratory for their help in obtaining data. We would also like to thank Benoit Camenen for his meaningful input on the first draft of this manuscript.

References

Ang, R., Kinouchi, T., and Zhao, W.: Evaluation of daily gridded meteorological datasets for hydrological modeling in data-sparse basins of the largest lake in Southeast Asia, J. Hydrol.: Reg. Stud., 42, 101 135, https://doi.org/10.1016/j.ejrh.2022.101135, 2022.

Beck, H. E., Vergopolan, N., Pan, M., Levizzani, V., van Dijk, A. I. J. M., Weedon, G. P., Brocca, L., Pappenberger, F., Huffman, G. J., and Wood, E. F.: Global-scale evaluation of 22 precipitation datasets using gauge observations and hydrological modeling, Hydrol. Earth Syst. Sci., 21, 6201–6217, https://doi.org/10.5194/hess-21-6201-2017, 2017.

Beck, H. E., Pan, M., Roy, T., Weedon, G. P., Pappenberger, F., van Dijk, A. I. J. M., Huffman, G. J., Adler, R. F., and Wood, E. F.: Daily evaluation of 26 precipitation datasets using Stage-IV gauge-radar data for the CONUS, Hydrol. Earth Syst. Sci., 23, 207–224, https://doi.org/10.5194/hess-23-207-2019, 2019a.

Beck, H. E., Wood, E. F., Pan, M., Fisher, C. K., Miralles, D. G., van Dijk, A. I. J. M., McVicar, T. R., and Adler, R. F.: MSWEP V2 Global 3-Hourly 0.1° Precipitation: Methodology and Quantitative Assessment, Bull. Am. Meteorol. Soc., 100, 473–500, https://doi.org/10.1175/BAMS-D-17-0138.1, 2019b.

Binh, L. T. H., Umamahesh, N. V., and Rathnam, E. V.: High-resolution flood hazard mapping based on nonstationary frequency analysis: case study of Ho Chi Minh City, Vietnam, Hydrol. Sci. J., 64, 318–335, https://doi.org/10.1080/02626667.2019.1581363, 2019.

Bowman, W.: UTide, https://github.com/wesleybowman/UTide, 2020.

Calafat, F. M. and Marcos, M.: Probabilistic reanalysis of storm surge extremes in Europe, Proc. Natl. Acad. Sci. U.S.A., 117, 1877–1883, https://doi.org/10.1073/pnas.1913049117, 2020.

Caldwell, P. C., Merrifield, M. A., and Thompson, P. R.: Sea level measured by tide gauges from global oceans — the Joint Archive for Sea Level holdings (NCEI Accession 0019568), Dataset, Version 5.5, https://doi.org/10.7289/V5V40S7W, 2015.

Camenen, B., Dramais, G., Le Coz, J., Ho, T. D., Gratiot, N., and Piney, S.: Estimation of water level - slope - discharge rating curve for a tidal river, La Houille Blanche, 5, 16–21, https://doi.org/10.1051/lhb/2017039, 2017.

Camenen, B., Gratiot, N., Cohard, J.-A., Gard, F., Tran, V. Q., Nguyen, A.-T., Dramais, G., van Emmerik, T., and Némery, J.: Monitoring discharge in a tidal river using water level observations: Application to the Saigon River, Vietnam, Sci. Total Environ., 761, 143 195, https://doi.org/10.1016/j.scitotenv.2020.143195, 2021.

Cid, A., Camus, P., Castanedo, S., Méndez, F. J., and Medina, R.: Global reconstructed daily surge levels from the 20th Century Reanalysis (1871–2010), Global Planet. Change, 148, 9–21, https://doi.org/10.1016/j.gloplacha.2016.11.006, 2017.

Codiga, D. L.: Unified tidal analysis and prediction using the UTide Matlab functions, Graduate School of Oceanography, University of Rhode Island, Narragansett, RI, https://doi.org/10.13140/RG.2.1.3761.2008, 2011.

Couasnon, A., Scussolini, P., Tran, T. V. T., Eilander, D., Muis, S., Wang, H., Keesom, J., Dullaart, J., Xuan, Y., Nguyen, H. Q., Winsemius, H. C., and Ward, P. J.: A Flood Risk Framework Capturing the Seasonality of and Dependence Between Rainfall and Sea Levels—An Application to Ho Chi Minh City, Vietnam, Water Resour. Res., 58, e2021WR030 002, https://doi.org/10.1029/2021WR030002, 2022.

Dinh, C. S. and Nguyen, T. L.: Calculation re-assessment of flood frequency versus designed and considered climate change., 2019.

Duy, P. N., Chapman, L., Tight, M., Linh, P. N., and Thuong, L. V.: Increasing vulnerability to floods in new development areas: evidence from Ho Chi Minh City, Int. J. Clim. Change Strategies Manage., 10, 197–212, https://doi.org/10.1108/IJCCSM-12-2016-0169, 2017.

Farr, T. G., Rosen, P. A., Caro, E., Crippen, R., Duren, R., Hensley, S., Kobrick, M., Paller, M., Rodriguez, E., Roth, L., Seal, D., Shaffer, S., Shimada, J., Umland, J., Werner, M., Oskin, M., Burbank, D., and Alsdorf, D.: The Shuttle Radar Topography Mission, Rev. Geophys., 45, https://doi.org/10.1029/2005RG000183, 2007.

Gaborit, É., Anctil, F., Fortin, V., and Pelletier, G.: Hydro-meteorological evaluation of downscaled global ensemble rainfall forecasts, EGU General Assembly Conference Abstracts, pp. 2013–12 094, https://ui.adsabs.harvard.edu/abs/2013EGUGA..1512094G/abstract, 2013.

Haigh, I. D., MacPherson, L. R., Mason, M. S., Wijeratne, E. M. S., Pattiaratchi, C. B., Crompton, R. P., and George, S.: Estimating present day extreme water level exceedance probabilities around the coastline of Australia: tropical cyclone-induced storm surges, Clim. Dyn., 42, 139–157, https://doi.org/10.1007/s00382-012-1653-0, 2014.

Haigh, I. D., Wadey, M. P., Wahl, T., Ozsoy, O., Nicholls, R. J., Brown, J. M., Horsburgh, K., and Gouldby, B.: Spatial and temporal analysis of extreme sea level and storm surge events around the coastline of the UK, Sci. Data, 3, 1–14, https://doi.org/10.1038/sdata.2016.107, 2016.

Heidarzadeh, M., Teeuw, R., Day, S., and Solana, C.: Storm wave runups and sea level variations for the September 2017 Hurricane Maria along the coast of Dominica, eastern Caribbean sea: Evidence from field surveys and sea-level data analysis, Coastal Eng. J., 60, https://doi.org/10.1080/21664250.2018.1546269, 2018.

Hersbach, H., Bell, B., Berrisford, P., Hirahara, S., Horányi, A., Muñoz-Sabater, J., Nicolas, J., Peubey, C., Radu, R., Schepers, D., Simmons, A., Soci, C., Abdalla, S., Abellan, X., Balsamo, G., Bechtold, P., Biavati, G., Bidlot, J., Bonavita, M., De Chiara, G., Dahlgren, P., Dee, D., Diamantakis, M., Dragani, R., Flemming, J., Forbes, R., Fuentes, M., Geer, A., Haimberger, L., Healy, S., Hogan, R. J., Hólm, E., Janisková, M., Keeley, S., Laloyaux, P., Lopez, P., Lupu, C., Radnoti, G., de Rosnay, P., Rozum, I., Vamborg, F., Villaume, S., and Thépaut, J.-N.: The ERA5 global reanalysis, Q. J. R. Meteorolog. Soc., 146, 1999–2049, https://doi.org/10.1002/qj.3803, 2020.

Ho, L. P., Nguyen, T., Chau, N. X. Q., and Nguyen, K. D.: Integrated urban flood risk management approach in context of uncertainties: case study Ho Chi Minh city, La Houille Blanche, 100, 26–33, https://doi.org/10.1051/lhb/2014059, 2014.

Hoballah Jalloul, M., Scheiber, L., Jordan, C., Visscher, J., Nguyen, H. Q., and Schlurmann, T.: Uncovering Inundation Hotspots through a Normalized Flood Severity Index: Urban Flood Modelling Based on Open-Access Data in Ho Chi Minh City, Vietnam, https://doi.org/10.5194/nhess-2022-238, 2022.

Huang, C., Hu, J., Chen, S., Zhang, A., Liang, Z., Tong, X., Xiao, L., Min, C., and Zhang, Z.: How Well Can IMERG Products Capture Typhoon Extreme Precipitation Events over Southern China?, Remote Sens., 11, 70, https://doi.org/10.3390/rs11010070, 2019.

Huffman, G., Stocker, E., Bolvin, D., Nelkin, E., and Tan, J.: GPM IMERG Final Precipitation L3 1 day 0.1 degree x 0.1 degree V06, https://disc.gsfc.nasa.gov/datasets/GPM_3IMERGDF_06/summary?keywords=%22IMERG%20final%22, 2019.

Islam, Md. A. and Cartwright, N.: Evaluation of climate reanalysis and space-borne precipitation products over Bangladesh, Hydrol. Sci. J., 65, 1112–1128, https://doi.org/10.1080/02626667.2020.1730845, 2020.

Jiang, Q., Li, W., Fan, Z., He, X., Sun, W., Chen, S., Wen, J., Gao, J., and Wang, J.: Evaluation of the ERA5 reanalysis precipitation dataset over Chinese Mainland, J. Hydrol., 595, 125 660, https://doi.org/10.1016/j.jhydrol.2020.125660, 2021.

Jin, G., Pan, H., Zhang, Q., Lv, X., Zhao, W., and Gao, Y.: Determination of Harmonic Parameters with Temporal Variations: An Enhanced Harmonic Analysis Algorithm and Application to Internal Tidal Currents in the South China Sea, J. Atmos. Oceanic Technol., 35, 1375–1398, https://doi.org/10.1175/JTECH-D-16-0239.1, 2018.

Joyce, R. J., Janowiak, J. E., Arkin, P. A., and Xie, P.: CMORPH: A Method that Produces Global Precipitation Estimates from Passive Microwave and Infrared Data at High Spatial and Temporal Resolution, J. Hydrometeorol., 5, 487–503, https://doi.org/10.1175/1525-7541(2004)005<0487:CAMTPG>2.0.CO;2, 2004.

Khai, H. Q. and Koontanakulvong, S.: Impact of Climate Change on groundwater recharge in Ho Chi Minh City Area, Vietnam, https://www.researchgate.net/publication/275643904_Impact_of_Climate_Change_on_groundwater_recharge_in_Ho_Chi_Minh_City_Area_Vietnam, 2015.

660   Kidd, C. and Huffman, G.: Global precipitation measurement, Meteorol. Appl., 18, 334–353, https://doi.org/10.1002/met.284, 2011.

Larson, L. W. and Peck, E. L.: Accuracy of precipitation measurements for hydrologic modeling, Water Resour. Res., 10, 857–863, https://doi.org/10.1029/WR010i004p00857, 1974.

Le, T. A., Takagi, H., Heidarzadeh, M., Takata, Y., and Takahashi, A.: Field Surveys and Numerical Simulation of the 2018 Typhoon Jebi: Impact of High Waves and Storm Surge in Semi-enclosed Osaka Bay, Japan, Pure Appl. Geophys., 176, 4139–4160,
665   https://doi.org/10.1007/s00024-019-02295-0, 2019.

Leitold, R., Garschagen, M., Tran, V., and Revilla Diez, J.: Flood risk reduction and climate change adaptation of manufacturing firms: Global knowledge gaps and lessons from Ho Chi Minh City, Int. J. Disaster Risk Reduct., 61, 102 351, https://doi.org/10.1016/j.ijdrr.2021.102351, 2021.

Lin, N., Emanuel, K., Oppenheimer, M., and Vanmarcke, E.: Physically based assessment of hurricane surge threat under climate change,
670   Nat. Clim. Change, 2, 462–467, https://doi.org/10.1038/nclimate1389, 2012.

Marchesiello, P., Nguyen, N. M., Gratiot, N., Loisel, H., Anthony, E. J., Dinh, C. S., Nguyen, T., Almar, R., and Kestenare, E.: Erosion of the coastal Mekong delta: Assessing natural against man induced processes, Cont. Shelf Res., 181, 72–89, https://doi.org/10.1016/j.csr.2019.05.004, 2019.

Marchesiello, P., Kestenare, E., Almar, R., Boucharel, J., and Nguyen, N. M.: Longshore drift produced by climate-modulated monsoons and
675   typhoons in the South China Sea, J. Mar. Syst., 211, 103 399, https://doi.org/10.1016/j.jmarsys.2020.103399, 2020.

Mizukami, N. and Smith, M. B.: Analysis of inconsistencies in multi-year gridded quantitative precipitation estimate over complex terrain and its impact on hydrologic modeling, J. Hydrol., 428-429, 129–141, https://doi.org/10.1016/j.jhydrol.2012.01.030, 2012.

Munoz-Sabater, J., Dutra, E., Agusti-Panareda, A., Albergel, C., Arduini, G., Balsamo, G., Boussetta, S., Choulga, M., Harrigan, S., Hersbach, H., Martens, B., Miralles, D. G., Piles, M., Rodriguez-Fernandez, N. J., Zsoter, E., Buontempo, C., and Thepaut, J.-N.: ERA5-Land:
680   a state-of-the-art global reanalysis dataset for land applications, Earth Syst. Sci. Data, 13, 4349–4383, https://doi.org/10.5194/essd-13-4349-2021, 2021.

Ngoc, T. A., Hiramatsu, K., and Harada, M.: Optimizing the rule curves of multi-use reservoir operation using a genetic algorithm with a penalty strategy, vol. 12, pp. 125–137, Springer Japan, https://doi.org/10.1007/s10333-013-0366-2, 2014.

Ngoc, T. D. T., Perset, M., Strady, E., Phan, T. S. H., and Gratiot, N.: Ho Chi Minh City growing with waterre-
685   lated challenges, UNESCO/ARCEAU IdF, https://www.researchgate.net/publication/318759189_Ho_Chi_Minh_City_growing_with_waterrelated_challenges, 2016.

Nguyen, A. T., Némery, J., Gratiot, N., Dao, T.-S., Le, T. T. M., Baduel, C., and Garnier, J.: Does eutrophication enhance greenhouse gas emissions in urbanized tropical estuaries?, Environ. Pollut., 303, 119 105., https://doi.org/10.1016/j.envpol.2022.119105, 2022.

Nguyen, K.-A., Liou, Y.-A., and Terry, J. P.: Vulnerability of Vietnam to typhoons: A spatial assessment based on hazards, exposure and
690   adaptive capacity, Sci. Total Environ., 682, 31–46, https://doi.org/10.1016/j.scitotenv.2019.04.069, 2019a.

Nguyen, T., Némery, J., Gratiot, N., Strady, E., Tran, V. Q., Nguyen, A. T., Aimé, J., and Peyne, A.: Nutrient dynamics and eutrophication assessment in the tropical river system of Saigon – Dongnai (southern Vietnam), Sci. Total Environ., 653, 370–383, https://doi.org/10.1016/j.scitotenv.2018.10.319, 2019b.

Nguyen, T. T. N., Nemery, J., Gratiot, N., Garnier, J., Strady, E., Nguyen, D. P., Tran, V., Nguyen, A. T., Cao, S. T., and Huynh, T. P. T.:
695   Nutrient budgets in the Saigon-Dongnai River basin: Past to future inputs from the developing Ho Chi Minh megacity (Vietnam), River Res. Appl., https://hal.archives-ouvertes.fr/hal-02436346, 2020.

NOAA: Storm Surge, https://www.nhc.noaa.gov/surge, 2023.

Orton, P. M., Talke, S. A., Jay, D. A., Yin, L., Blumberg, A. F., Georgas, N., Zhao, H., Roberts, H. J., and MacManus, K.: Channel Shallowing as Mitigation of Coastal Flooding, J. Mar. Sci. Eng., 3, 654–673, https://doi.org/10.3390/jmse3030654, 2015.

700 Parker, B. B.: Tide Analysis and Prediction, https://tidesandcurrents.noaa.gov/publications/Tidal_Analysis_and_Predictions.pdf, 2007.

Phan, D. C., Trung, T. H., Truong, V. T., Sasagawa, T., Vu, T. P. T., Bui, D. T., Hayashi, M., Tadono, T., and Nasahara, K. N.: First comprehensive quantification of annual land use/cover from 1990 to 2020 across mainland Vietnam, Sci. Rep., 11, 9979., https://doi.org/10.1038/s41598-021-89034-5, 2021.

Pugh, D.: Changing Sea Levels: Effects of Tides, Weather and Climate, Cambridge University Press, Cambridge, England, UK, https:
705 //books.google.fr/books/about/Changing_Sea_Levels.html?id=Ysa4ymmEotYC&redir_esc=y, 2004.

Pugh, D. and Woodworth, P.: Sea-level science: Understanding tides, surges, tsunamis and mean sea-level changes, Cambridge University Press, https://doi.org/10.1017/CBO9781139235778, 2012.

Rujner, H. and Goedecke, M.: Urban Water Management: Spatial Assessment of the Urban Water Balance, in: Sustainable Ho Chi Minh City: Climate Policies for Emerging Mega Cities, pp. 133–150, Springer, Cham, Switzerland, https://doi.org/10.1007/978-3-319-04615-
710 0_8, 2016.

Sakamoto, T., Van Nguyen, N., Kotera, A., Ohno, H., Ishitsuka, N., and Yokozawa, M.: Detecting temporal changes in the extent of annual flooding within the Cambodia and the Vietnamese Mekong Delta from MODIS time-series imagery, Remote Sens. Environ., 109, 295–313, https://doi.org/10.1016/j.rse.2007.01.011, 2007.

Schwarzer, K., Thanh, N. C., and Ricklefs, K.: Sediment re-deposition in the mangrove environment of Can Gio, Saigon River estuary
715 (Vietnam), J. Coast. Res., 75, 138–142, https://doi.org/10.2112/SI75-028.1, 2016.

Sebastian, M., Behera, M. R., and Murty, P. L. N.: Storm surge hydrodynamics at a concave coast due to varying approach angles of cyclone, Ocean Eng., 191, 106 437, https://doi.org/10.1016/j.oceaneng.2019.106437, 2019.

Takagi, H., Thao, N. D., and Esteban, M.: Tropical Cyclones and Storm Surges in Southern Vietnam, in: Coastal Disasters and Climate Change in Vietnam, pp. 3–16, Elsevier, Walthm, MA, USA, https://doi.org/10.1016/B978-0-12-800007-6.00001-0, 2014.

720 Thuan, D. H., Binh, L. T., Viet, N. T., Hanh, D. K., Almar, R., and Marchesiello, P.: Typhoon Impact and Recovery from Continuous Video Monitoring: a Case Study from Nha Trang Beach, Vietnam, J. Coast. Res., 75, 263–267, https://doi.org/10.2112/SI75-053.1, 2016.

Thuy, N. B., Kim, S., Chien, D. D., Dang, V. H., and Hole, L. R.: Assessment of Storm Surge along the Coast of Central Vietnam, J. Coast. Res., 33, https://doi.org/10.2112/JCOASTRES-D-15-00248.1, 2016.

Thuy, V.: Storm surge modelling for Vietnam's coast, Master's Thesis, IHE Delft: Delft, The Netherlands, p. 140, https://www.
725 semanticscholar.org/paper/Storm-surge-modelling-for-Vietnam:%27s-coast-Thuy/03d4d0a4dde472a8e98a051776d61a5a0d6f883e, 2003.

Trinh, T. T., Pattiaratchi, C., and Bui, T.: The Contribution of Forerunner to Storm Surges along the Vietnam Coast, J. Mar. Sci. Eng., 8, 508, https://doi.org/10.3390/jmse8070508, 2020.

Tu, T. A., Tweed, S., Dan, N. P., Descloitres, M., Quang, K. H., Nemery, J., Nguyen, A., Leblanc, M., and Baduel, C.: Local-
730 ized recharge processes in the NE Mekong Delta and implications for groundwater quality, Sci. Total Environ., 845, 157 118, https://doi.org/10.1016/j.scitotenv.2022.157118, 2022.

Vachaud, G., Quertamp, F., Phan, T. S. H., Tran Ngoc, T. D., Nguyen, T., Luu, X. L., Nguyen, A. T., and Gratiot, N.: Flood-related risks in Ho Chi Minh City and ways of mitigation, J. Hydrol., 573, 1021–1027, https://doi.org/10.1016/j.jhydrol.2018.02.044, 2019.

Vachaud, G., Gratiot, N., and Tran Ngoc, T. D.: Ho Chi Minh Ville, des inondations à la submersion..., EchoGéo, https://journals.
735 openedition.org/echogeo/19473, 2020.

Williams, J., Horsburgh, K. J., Williams, J. A., and Proctor, R. N. F.: Tide and skew surge independence: New insights for flood risk, Geophys. Res. Lett., 43, 6410–6417, https://doi.org/10.1002/2016GL069522, 2016.

Xiang, Y., Chen, J., Li, L., Peng, T., and Yin, Z.: Evaluation of Eight Global Precipitation Datasets in Hydrological Modeling, Remote Sens., 13, 2831, https://doi.org/10.3390/rs13142831, 2021.

740   Ziese, M., Rauthe-Schöch, A., Becker, A., Finger, P., Rustemeier, E., and Schneider, U.: GPCC Full Data Daily Version 2020 at 1.0°: Daily Land-Surface Precipitation from Rain-Gauges built on GTS-based and Historic Data, https://opendata.dwd.de/climate_environment/GPCC/html/fulldata-daily_v2020_doi_download.html, 2020.